AD_____

Award Number: DAMD17-01-1-0110

TITLE: Molecular Determinants of Radio Resistance in Prostate Cancer

PRINCIPAL INVESTIGATOR: Robert G. Bristow, Ph.D., M.D.

CONTRACTING ORGANIZATION: University Health Network, Toronto
Toronto, Ontario
Canada M5G 2C4

REPORT DATE: August 2003

TYPE OF REPORT: Annual

PREPARED FOR: U.S. Army Medical Research and Materiel Command
Fort Detrick, Maryland 21702-5012

REPORT DOCUMENTATION PAGE

Form Approved
OMB No. 074-0188

1. AGENCY USE ONLY (Leave blank)	2. REPORT DATE	3. REPORT TYPE AND DATES COVERED
	August 2003	Annual (1 Aug 2002 - 31 Jul 2003)

4. TITLE AND SUBTITLE
Molecular Determinants of Radio Resistance in Prostate Cancer

5. FUNDING NUMBERS
DAMD17-01-1-0110

6. AUTHOR(S)
Robert G. Bristow, Ph.D., M.D.

7. PERFORMING ORGANIZATION NAME(S) AND ADDRESS(ES)
University Health Network, Toronto
Toronto, Ontario
Canada M5G 2C4

E-Mail: rob.bristow@rmp.uhn.on.ca

8. PERFORMING ORGANIZATION REPORT NUMBER

9. SPONSORING / MONITORING AGENCY NAME(S) AND ADDRESS(ES)
U.S. Army Medical Research and Materiel Command
Fort Detrick, Maryland 21702-5012

10. SPONSORING / MONITORING AGENCY REPORT NUMBER

11. SUPPLEMENTARY NOTES
Original contains color plates: All DTIC reproductions will be in black and white.

12a. DISTRIBUTION / AVAILABILITY STATEMENT
Approved for Public Release; Distribution Unlimited

12b. DISTRIBUTION CODE

13. ABSTRACT (Maximum 200 Words)
We are studying the radiation response of prostate tissues in relation to the sensing and repair of DNA breaks. Specific aims relate to determining the interaction of DNA repair proteins in vitro using immunoflorescent confocal microscopy and biochemical DNA rejoining assays under both hypoxic and oxic conditions (given in vivo tumour cell populations). An in vivo program of prostate xenograft radioresponse and patient biopsy studies will determine the level of DNA repair in situ using immunohistochemistry and immunoflorescent markers. Our studies show that DNA repair protein expression is abnormal in malignant versus normal prostate epithelial cultures, and that particularly the Rad51 protein is defective in localizing to the nucleus following DNA damage. We have accrued 13 patients onto a pre-operative radiotherapy trial and all patients' tumours are p53 wild type based on direct DNA sequencing. Post irradiation immunohistochemistry supports an induction of p53-pathway signaling following 25Gy in 5 fractions of clinical radiotherapy. Current experiments are designed to determine whether DNA protein focal interactions using 2-phtoon microscopy can predict the radioresponse of prostate xenografts and human tumors, in vivo. Our studies support the use of novel molecular based therapies that target NDA repair for prostate cancer therapy.

14. SUBJECT TERMS
Prostate cancer, DNA repair, xenografts, cell death

15. NUMBER OF PAGES
50

16. PRICE CODE

17. SECURITY CLASSIFICATION OF REPORT	18. SECURITY CLASSIFICATION OF THIS PAGE	19. SECURITY CLASSIFICATION OF ABSTRACT	20. LIMITATION OF ABSTRACT
Unclassified	Unclassified	Unclassified	Unlimited

Table of Contents

Introduction:

The current funded study entitled "Molecular mechanisms of radioresistance in prostate cancer", is investigating the role of DNA break repair in the radiation response of normal and malignant prostate epithelium. The overall hypothesis of this project is that the radiation response of normal and cancerous prostate tissues can be correlated to the appropriate sensing and repair of DNA breaks by repair complexes following exposure to ionizing radiation. Specific aims relate to determining the interaction of DNA repair proteins in vitro using immunoflorescent confocal microscopy and biochemical DNA rejoining assays under both hypoxic and oxic conditions (given in vivo tumour cell populations). An in vivo program of prostate xenograft radioresponse is also being initiated to determine the level of DNA repair *in situ* using immunohistochemistry and immunoflorescent markers. These initial studies will determine the heterogeneity in fractionated response in a series of prostate xenografts as relates to DNA repair capacity, which may be translated to novel markers for radiation response in patients who receive prostate radiation therapy. The relevance of this project is that this *in vitro* to *in vivo* pre-clinical approach may derive clinical biomarkers of radiation response which can predict which patients will most benefit from radiation therapy for prostate cancer. The project will also determine the molecular mechanisms behind radiation response, in general, in prostate epithelial tissues.

Body:

Task 1: Initally, the first task was to primarily complete in vitro studies on PC-3; LNCaP, DU145 and normal prostate (PRSE and PREC) cells relating to DNA double strand break repair. Clonogenic radiation curves were derived for all 5 cell cultures and after detailed studies, terminal growth arrest and not apoptosis was found to be responsible for cell kill. This was important as it supportedour grant's hypothesis that DNA repair is an important endpoint for study as it correlates more to cell survival using terminal growth arrest or cell senescence. For example, in all 5 cell lines, we found that there was an increase in the p16 superscript ink4a and $p21^{WAFWAF}$ genes at 5-9 days following 2-10 Gy of ionizing radiation. Furthermore, these cells were found to contain senescent populations which was quantitated and found to be dose responsive and correlated to their clonogenic survival (using a novel fluorescent flow cytometric proliferation assay). This work has been published in ***Prostate Cancer and Prostate Diseases (see Appendix)***.
THIS SUB-TASK IS NOW COMPLETE

Task one projects were also completed for all 5 cell lines in determining the ability for the cells to repair double strand breaks, single strand breaks and DNA base damage (and oxidative damage) following ionizing radiation using the comet assay. We observed a series of novel observations which currently suggests that malignant prostate cancer cells have a DNA repair defect in the repair of DNA-dsbs, DNA-ssbs and DNA-base damage and oxidative damage in relation to the two normal prostate epithelial and stromal cell cultures. **This has not been reported before.** This repair can be altered under hypoxic conditions and affect DNA-dsb repair protein expression; new studies are warranted in separate grants to follow up this observation. **THIS SUB-TASK IS NOW COMPLETE and a manuscript is being written.**

RNA protection and Western blot analyses suggest that that the non-homologous (ie Ku70/80/DNA-PK) and homologous(ie rad50/51/XRCC3) proteins are upregulated at the transcriptional level in the malignant prostate cells compared to normal prostate cells (see Appendix 2; Fan et al). We therefore

went onto to discern protein function in terms of protein-protein interations during DNA repair as outlined in our previous annual report. Further quantitative confocal microscopy has shown that all though the 3 malignant prostate epithelial cell lines (PC-3, DU-145, LNCaP) have high levels of protein expression on western blot analysis, they do not have functional RAD51 in terms of forming nuclear complexes following DNA damage. Further Western blot experiments suggest that the three malignant cells lines over-express proteins involved in the BER and SSB repair pathways-we are designing new experiments to test the functional significance of this overexpression. In terms of Rad51 and homologous recombination(HR) we believed that there might be mutations in the Rad51, BRCA2 and BRCA1 genes to account for this finding; but mutational analyses and protein truncation assays suggest that in all 5 cells lines, these genes are wild type-suggesting a defect in intracellular trafficking for Rad51 in malignant cells which may explain the decreased intranuclear function. New experiments are being designed to test whether Rad51 translocation is modified by sumoylation, ubiquitination or phosphorylation and will be the subject of a new separate grant application. We are also determining the relative levels of HR by scoring chromosome versus chromatid aberrations following IR and MMC to determine whether faulty Rad51 translocation correlates with increased chromatid aberrations. **Such data has not been published before and a draft manuscript is appended with respect to the Rad51 defect data. THIS SUB-TASK IS NOW COMPLETE.**

Primary prostatic cultures were initiated as prostatectomy specimen cultures available through Coriell Laboratories. We were successful in culturing both the prostate stromal and the prostate epithelial cell cultures in vitro to be utilized in a radiobiology and DNA repair experiments. DNA double stand break repair complexes have been determined in these cultures and are part of the data set contained in the manuscript in Appendix 1 and the manuscript in preparation, as noted above.

Xenografts from Erasmus University, Rotterdam were received after an MTA was signed and they were implanted into Balb/c mice for growth assays. An ethics approval for biopsies taken before and after 5 fraction (25 Gy in 5 fractions pre-operative radiotherapy) during clinical prostate radiotherapy was given by our research ethics board (REB) and this was submitted to the US Army as part of the documentation for this grant. We now have increased to 12 patients which have been accrued to the phase 1 pilot study of preoperative radiotherapy, and we are using both pre and post radiotherapy biopsies on these patients to derive the markers related to in vivo irradiation or patient irradiation as outlined in Tasks 2 and 3. **We have therefore completed all endpoints for Task 1.**

Task 2: Complete in vivo radiobiologic studies on human prostate xenografts (months 12-24).

We have determined that there are cell cycle phase specific changes in Rad51 or H2AX foci formation in relation to DNA-dsb rejoining, by irradiating cells under both asynchronous and G0-G1 synchronized conditions. Counterstaining with PCNA and CENP-F is ongoing and will determine whether foci are specifically forming in a cell-cycle phase specific manner in malignant prostate cells versus normal cells in vitro. We expect this will be completed within 6 months.

Single dose and fractionated experiments have been completed for the PC-3 and the selected Rotterdam xenografts, utilizing the dose of 20 Gy, and then the xenografts were removed and stained for immunohistochemical markers pertaining to p53, apoptosis related genes (bax, BCL2 and TUNEL assay as well as survivin) and DNA repair markers (RAD50, BRCA1, BRCA2, RAD50, $DNAPK_{cs}$, KU70, KU80, ATM, P21, RB, MYC and RPA). The xenograft histology was also stained for proliferation

markers such as MIB-1, KI-67 and PCNA. Our results continue to suggest that RAD51 and RAD50 and BRCA2 increase in expression both in terms of the nuclear intensity of staining as well as a number of cells positively staining for protein following 20 Gy or irradiation *in vivo* at 24 hours.. **This has not been reported in the literature before.**. Rad51 staining in hypoxic areas as determined with EF-5 and CA-IX, is decreased suggesting an inverse relationship between HR-related DNA repair proteins and hypoxia. This may explain in part hypoxia-mediated genetic instability. **THIS SUB-TASK IS COMPLETE** and we are scoring the final data for a manuscript.

Unlike *in vitro* experiments, the observation of discrete DNA repair foci using normal microscopic IHC within histologic specimens of xenografts irradiated *in vivo* have been difficult and does not have the resolution of the confocal microscopy. We are attempting to utilize 2-photon microscopy for better resolution of the innate foci with indirect immunofluorescence.

We have increased the total number of patients accrued to the preoperative radiotherapy study from 6 to 13. Accrual will be complete at 15 patients and this sub-task is complete. We have sequenced all patients for their p53 gene status for all 11 exons and all patients are wild-type for p53. Immunohistochemistry for p53, p21, TUNNEL, Bax, Bcl-2, BRCA1/2/Rad51/DNA-PKcs/KU70/KU80 and PCNA is completed and we are quantitating the staining pre and post-radiotherapy using the Image Pro Plus analysis program. Final data analyses should be complete within 3 months for the writing of a manuscript. We have confirmed upregaultion of the p53-responsive p21WAF gene in irradiated prostate patients for the first time. **THIS SUB-TASK IS ALMOST COMPLETE.**

Unfortunately, due to a contamination of our animals from our supplier with *Pseudomonas Aeruginosa,* our entire colony of mice (greater than 70 animals) bearing Rotterdam-xenografts had to be sacrificed before we could complete in vivo fractionation experiments. Although our facility was not in any way at fault, this has set the xenograft program back by 8-10 months. **THIS SUB-TASK IS INCOMPLETE. DUE TO THE NATURE OF THE PROBLEM, WE WILL BE THEREFORE ASKING FOR A 12 MONTH EXTENSION TO THIS US ARMY GRANT** based on this first point and the effect that the SARS epidemic had on our Toronto-based research(see below).

Task 3: (Months 18-36)

Task 3 is to primarily complete the clinical studies undergoing radiotherapy, and to determine DNA repair foci in human clinical biopsies pre and post radiotherapy in phase 3 and Phase 1 trials. Preliminary experiments are underway to test Rad51, BRCA2 and BRCA1 levels in tissue arrays containing normal, PIN and malignant prostate cancer specimens. **As stated above the Phase I trial is almost complete.** These studies are approximately 6 months behind due to decreased laboratory activities, patient appointments (and therefore accrual) during the period when our downtown-based Toronto hospital was affected by ***severe acute respiratory syndrome* (SARS).** All non-essential hospital activities, including research programs, out-patient clinics and meetings were halted for a period of 3 months from March to May, 2003. Partial quarantine measures continued through June and July, 2003 and but we are now back to our original momentum. **As such, this second factor will be the basis for asking for an extension to our grant until July, 2005**. Once the xenograft program is rebuilt we will continue our xenograft studies as it pertains to fractionated and single dose related growth delay experiments and DNA repair-associated markers. Some components of Task 3 will run long-term and parallel as patient biopsies are accrued for the assays.

KEY RESEACH ACCOMPLISHMENTS for YEAR 2:

1. DNA repair complexes can be visualized using confocal microscopy and quantitative and are dose dependant for the RAD50, H2AX and p53-ATM complexes. The appearance and disappearance of these foci correlate to the kinetics of DNA biochemical rejoining assays (ie. Comet assay).
2. Malignant prostate epithelium may have an effect has an inherent DNA defect in terms of DNA double strand break repair, single strand break repair and base damage repair. This is correlated to increased expression of proteins involved in each of these pathways (APE/REF1. RAD51, BRCA2, PARP, etc.). In the case of Rad51, altered expression is discordant from altered function and we believe that there is an intracellular trafficking defect in Rad51 related to post-translational modification.
3. Accrual to the phase I pilot study of preoperative radiotherapy has achieved in 13 patients. Immunohistochemical markers for DNA repair and apoptosis related proteins has been completed and are being objectively scored by an image analysis program. All patients are wild type for the p53 gene based on full-length automated DNA sequencing. Our IHC data supports that the p21WAF G1 checkpoint response is intact is patients given 25Gy in 5 fractions of pre-operative radiotherapy.

Reportable Outcomes:

Manuscripts:

Bromfield G, Fan R, Meng A, Kumaravel Ts, **Bristow RG**. Radiation-Induced Death Pathways in Prostate Cells: Role of Apoptotic and Non-Apoptotic Cell Death. Prostate Cancer and Prostate Diseases, 6: 73-85; 2003 (APPENDIX I).

Ma B, **Bristow RG**, Kim J, Siu L. Combined Modality Treatment of Solid Tumors Using Radiotherapy and Molecular Targeted Agents (Journal of Clinical Oncology, 21: 2760-2776; 2003.

Bayley AJ, Catton CN, Haycocks T, Kelly V, Alasti H, **Bristow R**, Catton P, Crook J, Gospodarowicz MK, McLean M, Milosevic M, Warde P. A Randomized Trial of Supine vs. Prone Positioning in Patients Undergoing Escalated Dose Conformal Radiotherapy for Prostate Cancer. (Radiotherapy and Oncology, In Press; October 2003).

Parker C, Milosevic M, Toi A, Sweet J, Panzarella T, Syed A, **Bristow R**, Catton C, Catton P, Crook J, Gospodarowicz M, Maclean M, Warde P, Hill R A polarographic electrode study of tumor oxygenation in localized prostate cancer; (Int J Radiat Oncol Biol Phys, In Press; October 2003).

Fan, R., Kumaravel, TS, Bromfield G.and **Bristow, R**. "Defective rad51 nuclear localization in malignant prostate cancer. DRAFT Manuscript (APPENDIX II)

Abstracts and Presentations:

Fan R, Kumaravel TS, Bromfield G, Jalali F, Meng A, **R. Bristow**. "DNA Repair in normal and malignant prostate epithelial tissues: implications for genetic stability and radiotherapy", ESTRO, Prague, September 2002.

Bristow RG, Fan R, Kumaravel TS, Bromfield G, Jalali F, Meng A. "DNA Repair in normal and malignant prostate epithelial tissues: implications for genetic stability and radiotherapy", CARO, Toronto, October 2002.

Bristow RT, Fan R, Kumaravel TS, Al Rashid S, Jalali F, Bromfield G. "Homologous Recombination as A Target for Therapy in Prostate Cancer". GRC on Radiation Oncology, California, January 2003.

Bristow R, Fan R, Kumaravel TS, Jalali F, Bromfield G. ICTRR 2003 Conference. "Aberrant Rad51 Function in Prostate Cancer Cell Lines: Basis for Radiotherapy Prediction and Novel Therapy". Lugano, March 2003.

Bristow R. "Rad51 as target in prostate cancer treatment". 2nd Annual CPC-BioNet Satellite Meeting. Montreal, June 2003.

Invited Lectures-R. Bristow:

Bristow R. "Cancer Genetics and Individualized Cancer Treatment: Lessons with Prostate Cancer", Invited Speaker, Ontario Medical Student Weekend Conference, November 2002.

Bristow R. "DNA repair: from cellular and molecular to clinical syndromes" Invited Speaker. 2nd Radiobiology Workshop. Nijmegen, The Netherlands. June 1-3, 2003.

Other reportable outcomes:

There is continued development of the tissue bank relating to irradiated prostate specimens as it relates to the phase I and phase III clinical trials; the latter has accumulated 170 biopsies of patients having undergone radical radiotherapy at PMH-UHN. Our REBs has been re-approved for all human studies. Funding was applied to the Ontario Cancer Research Network (OCRN) to test anti-sense to Rad51 as an experimental prostate therapy, based on our Rad51-overexpression data from this US Army grant. We were successful and received a grant totaling more than $ 420,000 CAN for pre-clinical studies based on the data derived from our US Army grant.

Dr. Rong Fan, a post doctoral fellow recruited following a previous post-doctoral fellowship at Harvard University, was supported by this US Army award. She did extremely well in her studies relating to RAD51 and is first author on 2 manuscripts in preparation; she has been hired by another laboratory and continues in science.

Conclusions:

Although our momentum slowed due to SARS and the animal colony contamination as mentioned above, we have made further headway in some of the TASKS regarding the importance of DNA-dsb repair as an important endpoint in the radiation response of prostate cancer and potentially, prostate carcinogenesis. Out studies suggest that there are defects in DNA repair relating not to mutation, but rather inappropriate intracellular trafficking or chaperoning of DNA repair factors to the nucleus. This is a novel concept and could give rise to new treatments targeting nuclear import and export of proteins in prostate cancer. Other DNA repair pathways amenable to study and targeting are the DNA-ddb and base

excision repair (BER) pathways which also are abnormal in prostate cancer cells. Our data with human biopsies pre and post-clinical radiotherapy also supports the quantification of DNA damage signaling pathways and repair factors as potential determinants of radioresponse.

Prostate Cancer and Prostatic Diseases (2003) 6, 73–85
 1365-7852/03 $25.00
www.nature.com/pcan

Cell death in irradiated prostate epithelial cells: role of apoptotic and clonogenic cell kill

GP Bromfield[2], A Meng[2], P Warde[1] & RG Bristow[1,2*]

[1]*Department of Radiation Oncology, University of Toronto and the Ontario Cancer Institute/Princess Margaret Hospital, University Health Network, Toronto, Ontario, Canada; and* [2]*Department of Medical Biophysics, University of Toronto, Toronto, Ontario, Canada*

Dose-escalated conformal radiotherapy is increasingly being used to radically treat prostate cancer with encouraging results and minimal long-term toxicity, yet little is known regarding the response of normal or malignant prostate cells to ionizing radiation (IR). To clarify the basis for cell killing during prostate cancer radiotherapy, we determined the IR-induced expression of several apoptotic- (bax, bcl-2, survivin and PARP) and G1-cell cycle checkpoint- (p53 and $p21^{WAF1/Cip1}$) related proteins, in both normal (PrEC-epithelial and PrSC-stromal) and malignant (LNCaP, DU-145 and PC-3; all epithelial) prostate cells. For these experiments, we chose doses ranging from 2 to 10 Gy, to be representative of the 1.8–2 Gy daily clinical fractions given during curative radiotherapy and the 8–10 Gy single doses given in palliative radiotherapy. We observed that IR-induced bax and $p21^{WAF1/Cip1}$ protein expression were attenuated selectively in normal stromal and epithelial cell cultures, yet maintained their p53-dependency in malignant cell lines. For each cell culture, we also determined total apoptotic and overall radiation cell kill using a short-term nuclear morphologic assay and a long-term clonogenic survival assay, respectively. Clonogenic survival, as measured by the surviving fraction at 2 Gy (SF2), ranged from 0.05 (PrEC) to 0.55 (DU-145), suggesting that malignant prostate cells are more radioresistant than normal prostate cells, for this series. IR-induced apoptotic cell kill was minimal (less than 6% cell after a dose of 10 Gy at times of 24–96 h) and was not dose-dependent. Furthermore, apoptotic kill was not correlated with either molecular apoptotic response or clonogenic cell kill. Using a flow cytometric proliferation assay with the PrSC (stromal) and DU-145 (epithelial) representative cultures, we observed that a senescent-like phenotype (SLP) emerges within a sub-population of cells post-irradiation that is non-clonogenic. Terminal growth arrest was dose-responsive at 96 h following irradiation and associated with long-term expression of both $p21^{WAF1/Cip1}$ and $p16^{INK4a}$ genes. Future strategies for prostate radiotherapy prediction or novel treatments should additionally focus on terminal growth arrest as an important endpoint in prostate cancer therapy.
Prostate Cancer and Prostatic Diseases (2003) **6**, 73–85. doi:10.1038/sj.pcan.4500628

Keywords: prostate cancer; epithelium; senescence; apoptosis; radiosensitivity

Introduction

Dose-escalated (ie 76–80 Gy) radiotherapy is an important treatment option for men with intermediate-risk prostate cancer who present with T1 or T2 disease, a Gleason score greater than 6 out of 10 and serum prostatic specific antigen (PSA) values in the order of 10–20 μg/ml.[1] Successful radiotherapy results in a gradual decline of the serum PSA over 12–24 months following treatment where a PSA nadir of less than 1.0 μg/ml predicts for 5 year, long-term local control.[2] With three-dimensional conformal (3D-CRT) or intensity-modulated (IMRT) radiotherapy treatment protocols, 5 year PSA-free relapse rates are approximately 75–85% and associated with minimal late toxicity (less than 5%

*Correspondence to: RG Bristow, Department of Radiation Oncology, Princess Margaret Hospital (UHN), 610 University Avenue, Toronto, Ontario, Canada M5G 2M9.
E-mail: rob.bristow@rmp.uhn on.ca
Received 9 May 2002; revised 25 July 2002; accepted 7 August 2002

with Radiotherapy Oncology Group (RTOG) Grade 3–4 rectal or bladder damage).[2]

Yet these same data predict that 15–25% will not achieve local control following radical radiotherapy, thought in part to be due to the intrinsic radioresistance of prostate cancer cells secondary to genetic (eg apoptosis, cell-cycle or DNA-repair-related gene expression) or microenvironmental factors (eg hypoxia or altered growth factor expression).[3] The success of radiation therapy in prostate cancer treatment is therefore dependent on the eradication of all prostate tumor clonogens (ie tumor stem cells, estimated to be less than 1% of cells within a tumor), which are select tumor cells capable of unlimited proliferative potential. Failure to eradicate this particular population will result in the regrowth of the tumor following treatment.[4] Despite many advances towards understanding prostate carcinogenesis, little work has been published to date relating the mode of clonogenic cell kill following DNA damage in either normal and malignant prostate epithelial cell cultures. This information is important in defining new strategies to augment prostate cancer cell kill and understand the kinetics of cell kill following radiotherapy (in comparison to decreasing PSA value kinetics *in vivo*) and may allow optimal interpretation of post-radiotherapy biopsies as a secondary measure of local tumor control.

Apoptosis plays an important role in the death of both normal prostate and androgen-dependent malignant prostate tissue following androgen withdrawal, leading to a decrease in either glandular or tumor volume, respectively. This is supported by the observation of rapid apoptosis following castration in the rat prostate glands[5,6] (a response lacking in mice deficient in expression of the pro-apoptotic gene, bax[7]) and in patients treated with androgen-withdrawal therapy for locally advanced or metastatic prostate cancer.[8] The relationship between androgen ablation and apoptosis has led to a number of clinical studies that have attempted to determine whether local failure following radical radiotherapy is secondary to genetic factors that control radiation-induced apoptosis. However, taken together, clinicopathologic studies that have attempted to correlate altered expression of the p53, $p21^{WAF1/Cip1}$, bax, bcl-2 and caspase apoptosis-related genes and radiocurability have been inconclusive.[9,10] This may be due to small clinical sample size, differences in the quantitation or timing of immunohistochemical or gene expression endpoints,[11,12] variable clinical treatment parameters, or perhaps due to alternate mechanisms of prostate cell death that confound analyses focused solely on apoptotic endpoints.

Recent data has supported the hypothesis that apoptosis may not be the dominant mode of cell death following radio- and chemotherapy in stromal (ie fibroblast) and epithelial tissues.[13,14] Indeed, it has been suggested that in these and selected tumor models, apoptosis may actually occur in a non-clonogenic population following DNA damage.[15,16] Alternatively, a permanent cell-cycle arrest or senescence-like terminal growth arrest may also be a factor in determining prostate cell death following radiotherapy.[17] Markers of senescence, such as senescence-associated β-galactosidase (SA β-gal) activity and permanently elevated levels of $p21^{WAF1/Cip1}$ and $p16^{INK4a}$ are actively under investigation as biomarkers of terminal growth arrest in human tumors.[18] Chang and co-workers[19] observed that a number of DNA-damaging agents (including ionizing radiation) could induce a senescence-like phenotype (SLP) in 11/14 cell lines tested. Other laboratories[13] and reviews have outlined a number of considerations regarding radiation-induced cell-death, including cell-type dependency in defining the dominant mode(s) of death (ie apoptosis, mitotic-linked death and reproductive death (SLP)/necrosis).[20] An improved understanding of death processes has been afforded by novel flow cytometric methods to detect terminally-arrested tumor cells following drug treatment,[19,20] and ascertain their relative morphology and clonogenic potential.

The purpose of the current study was to examine the mode(s) of prostate cell death *in vitro* following exposure to ionizing radiation to possibly refine clinical biomarkers for prediction of radiotherapeutic response and suggest future treatment strategies. Apoptosis, proliferation and clonogenic survival were assessed in a panel of cell lines comprised of both normal (stromal-PrSC and epithelial-PREC) and malignant (LNCaP, DU-145, PC-3; all epithelial) cultures, to determine the overall cellular response. We demonstrate that apoptosis is not the dominant mode of cell kill in this panel of cell cultures post-IR. Instead, data on selected cell lines supports the concept that long-term proliferative arrest relates to clonogenic radiation cell killing *in vitro*.

Materials and methods

Cell culture

All cell cultures were incubated in vented tissue culture flasks under 5% CO_2 and 37°C culture conditions. LNCaP cells (a gift from L Chung, University of Virginia) were maintained in T-media (Gibco-BRL) and supplemented with 10% FCS. PC-3 and DU-145 cells were purchased from ATCC and maintained as suggested in Ham's F12K, and alpha-Modified Eagles Medium respectively, supplemented with 10% FCS and 2 mM L-glutamine. PrEC (normal prostate epithelial cells) and PrSC (normal prostate stromal cells) were purchased from Clonetics and maintained as per suggested protocol in PrEGM media and SCGM media, without testosterone supplementation, respectively. Both cell cultures have limited lifespan and proliferative potential in culture according to the supplier and we have consistently observed decreased growth rates following passage 5 *in vitro* for both cultures. Immortalized myc-infected Rat-1 HO15.19 fibroblast cells (a gift from Dr L Penn, OCI/PMH[21]) were maintained in Dulbecco's H21 media supplemented with 10% FBS. Cultures were maintained without testosterone supplementation to ensure that radiation survival studies were completed under similar conditions in normal and malignant prostate cultures and as previous experiments have determined that exogenous testosterone may not always alter apoptotic responses, clonogenic survival or IR-induced $p21^{WAF1/Cip1}$ expression and cell arrest in androgen-*sensitive* cells (J Tsihlias, personal communication[22,23]) Approximate doubling times for cell cultures under these conditions were as follows: PrEC, 36–48 h (highly variable); PrSC, 18 h; LNCaP, 36 h; PC-3, 24 h; DU-145, 18 h; Myc-expressing Rat-1HO15.19, 16 h.

SF2Gy and clonogenic radiation survival curves

Logarithmically growing cells were rinsed with PBS/HBSS, trypsinized for 5 min at 37°C, and then were seeded at appropriate densities for colony formation in six-well dishes (Nunc). Asynchronous cultures were irradiated 16–20 h post-plating to reduce the immediate effects of trypsinization and such that the multiplicity index was less than 1.1.[24] At least two dilutions of cells in triplicate were used for each dose point for any given individual experiment. At least three independent clonogenic radiation experiments were completed for each cell line. Plated cells were either mock irradiated or irradiated with 0–10 Gy under aerobic conditions using a ^{137}Cs irradiator at ~1 Gy/min at room temperature. Plates were then incubated at 37°C for 7–14 days depending on cell doubling time *in vitro* and re-fed every 4–5 days before fixation and staining (methylene blue/50% methanol) of resulting colonies (aggregates of greater than 50 cells were scored as a colony). Radiation survival was calculated as the plating efficiency of treated cells divided by the plating efficiency of untreated cells and plotted as a function of dose on a semi-logarithmic plot as previously described.[24] We were unable to derive colonies at doses greater than 2 Gy in the LNCaP and PrEC cell cultures due to poor plating efficiencies, and therefore only SF2 values are presented for these cultures. For a given cell culture, there was no correlation between the SF2 values and plating efficiency amongst individual experiments, although mean SF2 values were increased in cell lines which exhibited increased plating efficiency, as reported in the literature (ie DU-145 and PC-3).[3,21]

Western blotting

Logarithmically-growing cells were irradiated and lysed on ice for 20 min with E7 lysis buffer as previously described.[24] Protein quantification was performed determined using a commercial Pierce-BCA assay kit to derive a mean concentration value based on three assays per lysate. SDS–PAGE was performed using 7–12% bis–acrylamide (29:1) gels with a 4% stacking gel run in a Novex X-cell semi-dry Mini Cell western blotting apparatus at room temperature. Each well was loaded with 20 μg of total protein plus loading buffer (final concentration 1×—6% glycerol, 0.83% β-mercaptoethanol, 1.71% Tris-HCl pH 6.8, 0.002% Bromophenol Blue) after boiling for 3 min. Samples resolved by electrophoresis at 80–110 V for 1.5–2.5 h were transferred onto nitrocellulose overnight at 14 V/4°C or for 1.5 h at 24 V/room temperature in transfer buffer (75 mM glycine, 10 mM Tris, 20% methanol). For selected blots, pre-hybridization staining with Ponceau S confirmed equal loading and transfer between running lanes.

To detect protein, membranes were blocked in TBST/0–10% low fat milk and then exposed to the primary antibody 2–4 h at room temperature constant rotation. Membranes were then rinsed with TBST and exposed to the appropriate secondary antibody for 1 h under similar conditions, rinsed again with TBST, once with 10× TBS and finally incubated in Amersham ECL chemiluminescence solution for 1 min. Membranes were exposed to Hyperfilm ECL from AmershamPharmacia and analyzed by densitometry (Molecular Dynamics Computing Densitometer, ImageQuant Mac version 1.2). Primary antibodies used in these studies included: p53-mouse monoclonal (Santa Cruz Bp53-12, 1:3000); $p21^{WAF1}$-mouse monoclonal (Oncogene Ab-1, 1:3000); Bax-rabbit polyclonal (Santa Cruz N-20, 1:1000); Bcl-2-mouse monoclonal (Santa Cruz 509, 1:500); PARP-mouse monoclonal (BioMol SA-249, 1:1000), survivin-rabbit polyclonal (Alpha Diagnostics SURV11, 1:5000), and $p16^{INK4A}$ mouse monoclonal (Oncogene Ab-1, 1:1000).

Assays for apoptotic cell death

Radiation-induced apoptosis was quantified on the basis of distinct nuclear morphology and associated apoptotic bodies based on a previously standardized immunofluorescence protocol (Hoechst 33342 staining).[24] For the morphology assay, logarithmically growing cells were re-plated at appropriate densities in triplicate and mock/irradiated with 0, 2, 10 or 20 Gy. These were scored for apoptotic morphology (ie apoptotic bodies and nuclear condensation—see sample in Figure 2a) at periods of 24–96 h following irradiation. Total adherent and floating cells in each culture were fixed and stained in 4% formalin-PBS/10 μM Hoechst 33342 DNA-specific dye for 30 min at RT. Cell counts to evaluate any cell loss/lysis into culture media were also performed at each time point. All experiments utilized Rat-1 HO15.19 cell line as positive control for gamma-irradiation induced apoptosis (L Penn, personal communication and Lee *et al*[25]).

Radiation survival in proliferating and non-proliferating irradiated cultures: the CFDA-SE flow cytometry proliferation assay

To determine if permanent arrest is associated with decreased clonogenic survival, a modification of the protocol by Chang *et al*[19] utilized the CFDA-SE (CFSE) fluorescent dye.[20,26] The CFSE compound (Molecular Probes, C-1157) is distributed throughout the cellular membranes and is divided evenly amongst subsequent progeny based on division of equal volumes of membrane at cell division. Multiple rounds of cell division are therefore represented by a corresponding decrease in total membrane fluorescence within a proliferating population, which can be detected by flow cytometry. Analyzing cell populations for relative fluorescence (FL1 (CFSE) parameter; increased non-proliferating cultures) and increasing side-scatter (SSC parameter; due to increased granularity associated with senescent cells) allows for flow cytometric analysis of senescent-like populations post-treatment.

Sub-confluent flasks of cells were trypsinized, collected and centrifuged into a pellet and 5×10^6 cells were re-suspended in 1 ml serum-free media plus 1 μl of stock solution (5 M CFSE in DMSO) at 37°C for 10 min with occasional inversion. Ice-cold RPMI 1640 + 10% FBS was then added prior to a subsequent cell centrifugation, and finally the cells were re-suspended in PBS. The cells were further washed twice in PBS, re-plated at low density (approximately 10% confluence) into multiple, 175 cm^2

Falcon flasks for next-day irradiation (0–10 Gy). As a control, all cells (floating and adherent) from one untreated flask were harvested one day post-plating and analyzed with flow cytometry to find baseline fluorescence (FL1(CFSE)) intensity. Remaining cultures were followed until day 5 when all cells (floating and adherent) were harvested, analyzed and sorted by FACS into 'non-proliferating' (FL1(CFSE)^{hi}SSC^{hi}), and 'proliferating' (ie all cells other than FL1(CFSE)^{hi}SSC^{hi}) populations to determine clonogenic potential within each population. The 5 day time point was initially chosen as it represents the point at wbich surviving cells would begin to show their colony-forming ability.[3] Sorted populations of DU-145 and PrSC were used to derive colonies in each sub-group as examples of epithelial and stromal (ie fibroblast-like) models. Pre-sort samples were analyzed on a BDIS FACScan analyzer and samples sorted using either a Becton Dickonson Immunocytometry system FACStarPLUS or BDIS FACS Vantage system. BDIS CELLQuest Software version 3.3 was used for both sorting and analysis. Cell lysates from adherent and floating cells in parallel cultures treated similarly (stained, irradiated with 0, 2 and 10 Gy) were also harvested on days 5–9, and analyzed for expression of the p16^{INK4a} and p21^{WAF1} genes. Cultures were also stained for senescence-associated β-galactosidase (SA β-gal) using the method of Chang *et al*,[19] as a complementary biomarker of senescence-like death.

Results

Gene expression of apoptosis-related genes within irradiated prostate cell cultures

As different laboratories may contain variants of original cell stocks, we initially determined the p53 status of the malignant prostate epithelial cell lines using full-length DNA sequencing of exons 1–11 of the p53 gene. Consistent with previous reports, LNCaP cells were found to express two wild-type (WT) alleles, whereas the PC-3 cells were devoid of p53 protein expression due to chromosome 17p hemizygosity and a mutation in the remaining allele at codon 138 which results in a premature stop codon at position 169. The DU-145 cells express mutant (MT) p53 protein due to mutations at codons 223 and 274. We observed that the level of bax protein expression is p53-dependent following IR, given the increased expression in the WTp53-expressing LNCaP cells at 24 h following 10 Gy. This molecular response was attenuated, or absent, in the remaining PC-3 and DU-145 malignant epithelial cell lines, which have altered p53 protein expression. Of note, despite the western blots shown in Figure 1b, bax expression is detectable in DU-145 cells, albeit at a very low level. The response was also attenuated within the normal epithelial and stromal cultures (see Figure 1a, b and Table 1). Bcl-2 protein levels were low, yet detectable, using our antibody, and remained unchanged in all cell cultures following 10 Gy for periods up to 24 h following radiation (see Figure 1c, d). In other experiments in our laboratory, the relative levels of bax and bcl-2 protein have been confirmed at the mRNA level by RNA protection analyses (R Fan and RG Bristow, manuscript in preparation). The IAP-related protein, survivin, has been suggested to be a prognostic indicator in a variety of cancers, presumably due to its influence on cellular apoptosis and G2 phase cell cycle control[27] and reported differential upregulation in malignant tissues, relative to normal tissues.[28] *In vitro*, endogenous survivin levels were observed to be detectable in all of the cell cultures within our series (normal and malignant), and were invariant following irradiation (Table 1) except for a slight (1.6-fold) increase in PrSC. Subsequent experiments have revealed lower levels of survivin in PrEC cultures than in their stromal and malignant counterparts.

Terminal apoptotic transduction involves altered expression and cleavage of the caspase family of proteins and the PARP protein.[29,30] Other laboratories have reported that caspase 1 and 3 protein expression can be deficient in some of our malignant cell lines.[31] In our experiments, analysis for PARP cleavage revealed that, although we detected an increase in the characteristic 89 kD a apoptotic-related PARP protein fragment in our highly apoptotic Rat-1 HO15.19 cell line, there was no such change in any of the five prostate cell cultures at 24 h following a dose of 10 Gy (data not shown). Our results (summarized in Table 1) suggest that gene and protein expression related to terminal apoptosis-defining events following IR is not consistent with observations made for other cells (eg lymphocytes or thymocyctes), which are classically more susceptible to radiation-induced apoptosis; however we recognize that the molecular apoptotic and morphologic (see below) response of our cell panel may be variable, depending on type of cell stress and drug treatment.

Minimal evidence of apoptotic cell death in irradiated prostate cultures

We next determined the level of radiation-induced apoptosis following various doses (2–20 Gy) and time points (0–96 h post-IR) using a distinct nuclear morphology assay (see Figure 2a) as previously described.[24] A dose of 10 Gy has been shown to decrease clonogenic survival by 3 logs or more, in other malignant cell lines. The highly apoptotic adherent Rat-1 HO15.19 cell line formed a positive control for IR-induced apoptosis in these experiments and irradiated cultures were observed to contain decreasing numbers of cells over 24–96 h consistent with a rapid induction of cell death (data not shown). The level of apoptosis in Rat-1 HO15.19 control following 20 Gy became difficult to quantify at 24 h due to a large amount of cellular debris and may be underestimated, as presented in Figure 2b. The apoptotic response of our prostate cell panel at times of 24–96 h following 10 Gy as determined by morphology is presented in Figure 2b, and reveals that neither normal nor malignant prostate cells undergo high levels of apoptosis at any time point up to 96 h (a time at which the earliest colonies indicative of clonogenic survival can be detected). Additionally, careful total cell counts of adherent and floating cells within all the irradiated cultures suggested that there was no decrease at any time point up to 96 h in total cell number, which ruled out underestimating apoptotic responses (data not shown). Moreover, in contrast to the

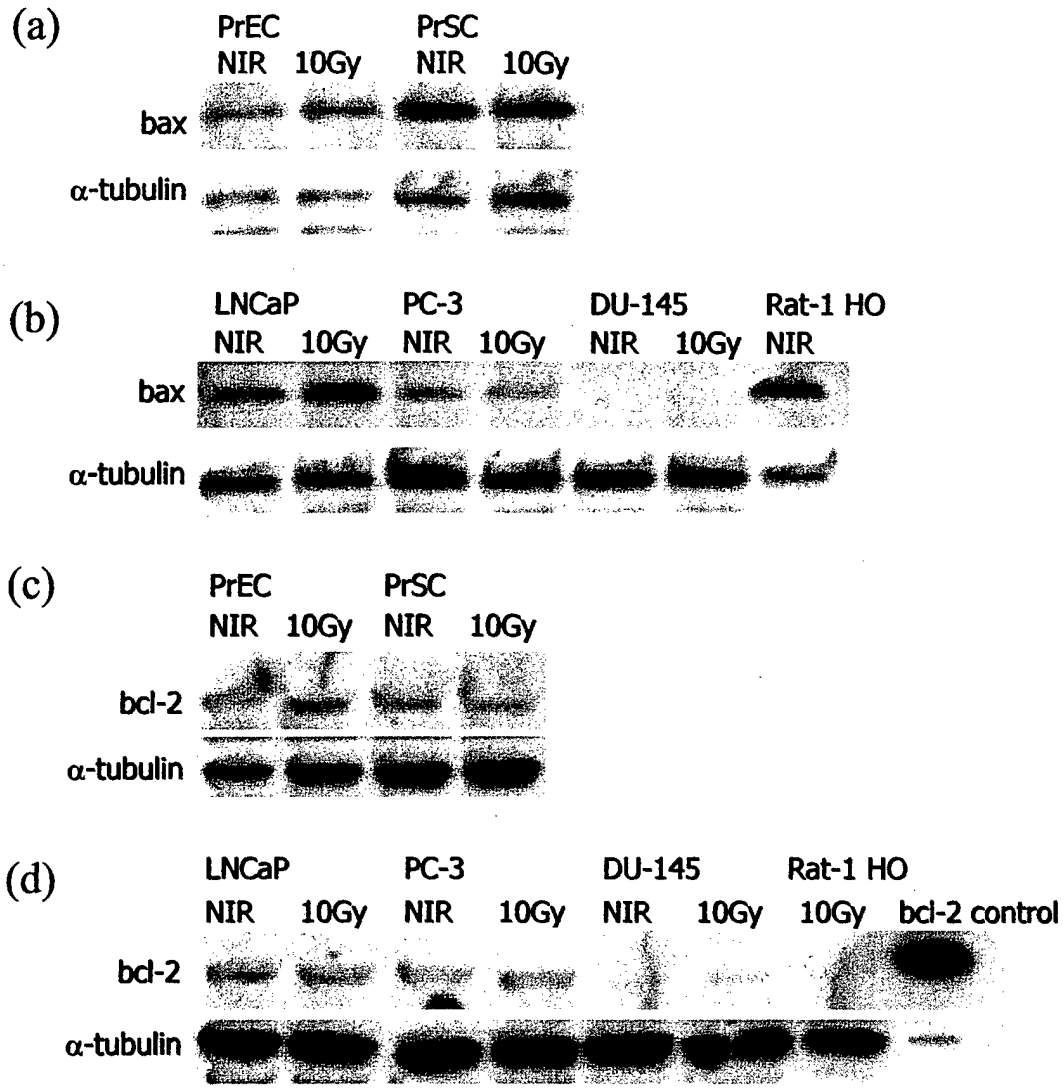

Figure 1 *Western blot analyses for apoptotic-related protein expression pre- and post-irradiation, in a panel of normal and malignant prostate cell cultures: (a) bax protein expression in normal prostate epithelial (PrEC) and stromal (PrSC) cell cultures; (b) bax protein expression in malignant prostate cell cultures (Rat-1 HO15.19 cell-lysate shown as positive control); (c) bcl-2 protein expression in normal prostate cell cultures; (d) bcl-2 protein expression in malignant prostate cell cultures (human bcl-2 transfected Rat-1 fibroblast lysate shown as positive control).*

Table 1 Apoptosis- and cell cycle-related gene expression in prostate cell cultures 24 h post-10 Gy irradiation, as compared to mock-irradiated controls

	p53	p21	bax	bcl-2	survivin
Normal					
PrEc	↑↑	↑	↔	↔	↔
PrSc	↑↑	↑↑	↔	↔	↔
Malignant					
LNCaP	↑↑	↑↑	↑↑	↔	↔
PC-3	n.d.*	Low[a]	↔	↔	↔
DU-145	↔	n.d.	n.d.	n.d.	↔

*n.d., non-detectable. [a]Low, barely detectable, no change post-XRT; ↔ less than 2-fold change; ↑ greater than 2-fold increase; ↑↑ greater than 4-fold increase (quantified using relative densitometry).

Rat-1 HO15.19 Myc-expressing control, there was no evidence for a dose-dependent increase in apoptosis in our panel of cultures (2 Gy range = 0–1%, 10 Gy range = 0–6%, 20 Gy range = 0–3%; see Figure 2c).

We observed a trend towards increased levels of apoptosis among the malignant cell lines as compared with the normal cell cultures, although these relative differences were not consistent. The data presented using the *in vitro* morphology assay was also supported by the absence of an apoptotic sub-G1[29] peak within DNA histograms of irradiated PC-3, DU-145 and LNCaP cells using flow cytometry, the lack of apoptotic morphology post-IR of the same cells as analyzed by the COMET DNA-damage assay,[32] and minimal TUNEL staining of the PC-3 cell line either *in vitro* or *in vivo* (growing as a xenograft i.m., in a nude mouse host) following irradiation (data not shown). These results suggest that cellular apoptosis is not a major mechanism of IR-induced prostate cell death under the culture and treatment conditions used in this study.

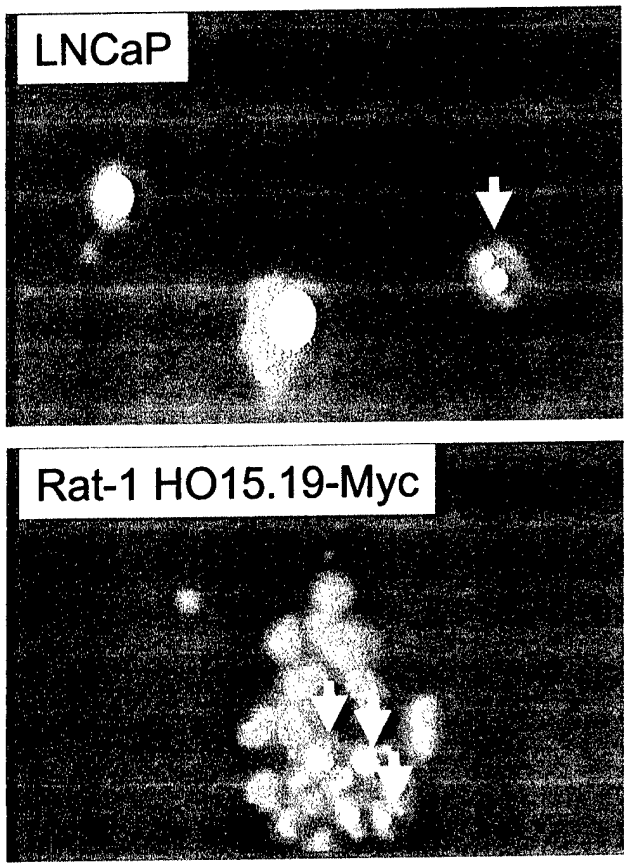

(a)

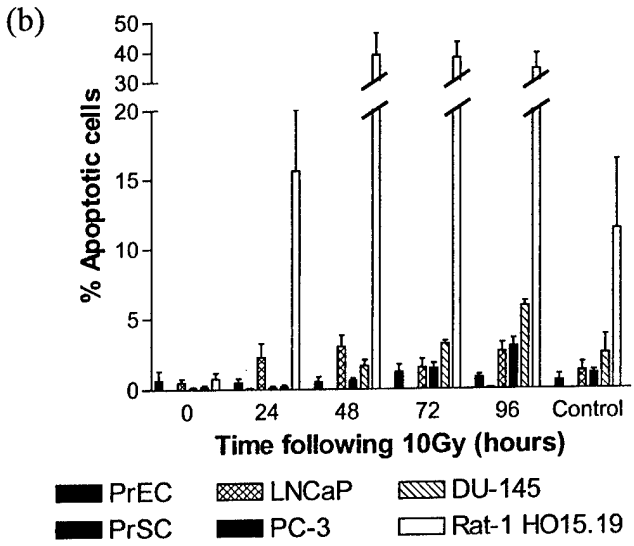

Figure 2 *IR-induced apoptosis in normal and malignant cell lines: (a) nuclear morphology of selected cell populations stained with Hoechst 33342 at 48 h following 10 Gy showing evidence of apoptotic bodies and chromatin condensation in cells denoted with white arrows: left panel, irradiated LNCaP cells; right panel, irradiated RAT-1 HO15.19 positive control cells (magnification 1000×); (b) time course of IR-induced apoptosis following a dose of 10 Gy (each bar represents the mean and s.e.m.); (c) dose-dependence of IR-induced apoptosis assayed at 48 h (error bars omitted for clarity in three-dimensional plot).*

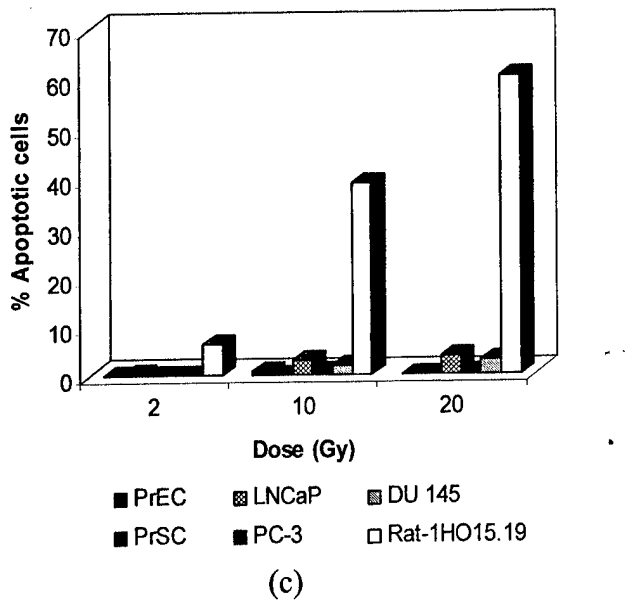

(c)

Figure 2 *(Continued).*

Molecular analysis of checkpoint control in prostate cells

The p53 status in normal and malignant cells can be functionally related to either apoptosis or a G1 and G2 cell cycle arrest or checkpoint, and dependent on cell type, level of DNA damage or cell stressor.[33,34] We therefore confirmed the presence or absence of a molecular p53-dependent G1 checkpoint in the normal and malignant prostate cells by determining the IR-induced upregulation of the cdk-inhibitory protein, $p21^{WAF1/Cip1}$. Following IR-induced DNA damage, the p53 protein is stabilized post-transcriptionally, by alternate phosphorylation of its amino terminus at serine residues 15 and 20 through both direct and indirect actions of the ATM protein. Stabilized p53 protein can then lead to a transcriptional upregulation of the $p21^{WAF1/Cip1}$ protein, which inhibits the G1 cyclin-cdk kinase complexes, and results in a G1 arrest secondary to hypo-phosphorylation of the pRB (retinoblastoma) protein. An increased level of p53 protein was observed following irradiation in all WTp53-expressing prostate cells and peaked at 2–6 h following IR-treatment (Figure 3). As expected, we observed a lack of p53 protein expression in irradiated null-p53 PC-3 cells and elevated endogenous levels of p53 protein in the MTp53-expressing DU-145 cells (consistent with a longer half-life for the MTp53 protein; Figure 3b), which were invariant post-IR. The PrEC and PrSC normal cultures both showed similar stabilization of the p53 protein relative to α-tubulin levels following irradiation. However, in the PrSC cells, the $p21^{WAF1/Cip1}$ levels were upregulated and sustained at 24 h; in the PrEC cells, the response was relatively attenuated in level and was duration reaching almost pre-irradiation levels at 24 h (Figure 3a). We failed to observe an increase in $p21^{WAF1/Cip1}$ expression in the MTp53-expressing and null-p53 cell lines (DU-145 and PC-3 respectively),[35] however the WTp53-expressing LNCaP cell line did show a strong IR-induced upregulation of $p21^{WAF1/Cip1}$.

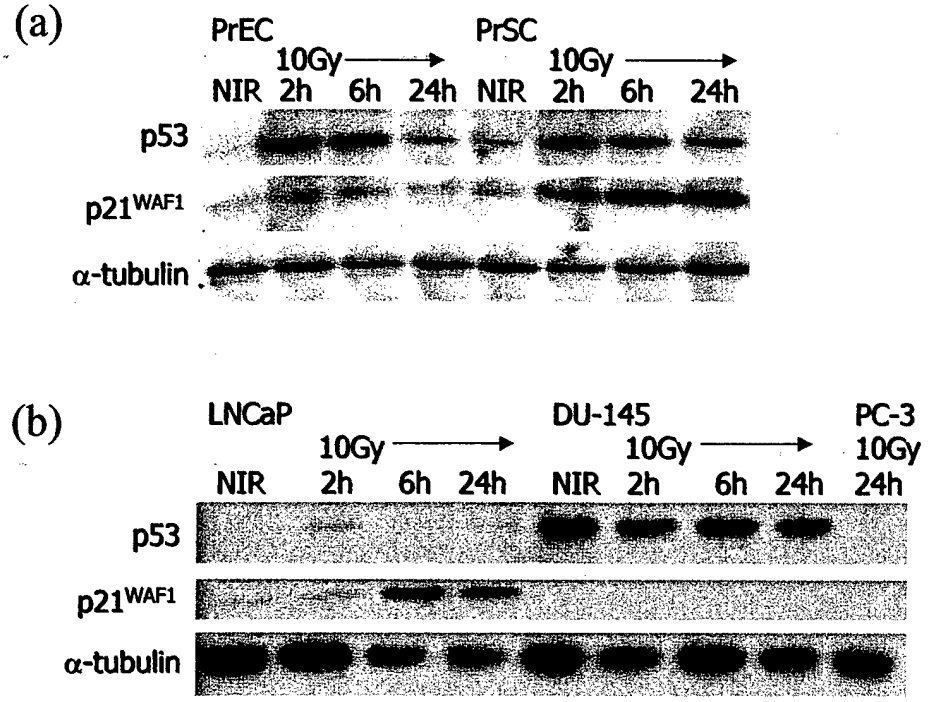

Figure 3 *Western blot analysis of p53 and p21$^{WAF1/Cip1}$ protein expression in (a) normal, and (b) malignant prostate cultures following 10 Gy irradiation.*

The p53 and p21$^{WAF1/Cip1}$ protein expression results were correlated to relative mRNA levels under similar culture conditions using RNA protection analyses in separate experiments (R Fan and RG Bristow, manuscript in preparation). These data support the idea that p53 can induce a molecular G1 checkpoint in both normal and malignant prostate epithelium, but highlights previous observations that, in certain normal epithelial cultures, p21$^{WAF1/Cip1}$ expression may be attenuated relative to stromal cultures[36] in a tissue-specific manner. This may relate to relative control of cell-cycle related checkpoint and carcinogenesis in these two tissues.[37]

SF2Gy and clonogenic survival for normal and malignant prostate cultures

Colony-formation after DNA damage measures the long-term survival of cells that are capable of unlimited proliferation and summarizes all types of IR-induced modes of cell death including apoptosis, mitotic-linked death (death after two or three aborted divisions followed by apoptosis or necrosis) and permanent growth arrest leading to necrosis.[33] Consistent with selected reports,[38,39] full clonogenic survival curves could not be generated for our LNCaP cell line, due to poor plating efficiencies, which made determination of colony-formation at doses greater than 2 Gy difficult. We encountered similar difficulties with PrEC normal epithelial cultures, which also had a poor plating efficiency (0.1–1%). Nonetheless, for all cell lines we were able to generate radiation survival data after a low, clinically relevant dose of 2 Gy (SF2), which approximates the daily fraction of radiation within curative radiation protocols. Full clonogenic survival curves following doses up to 10 Gy (a dose approximating a single-fraction palliative treatment) were derived for the PC-3, DU-145, PrSC and Rat-1 HO15.19 cell cultures and the results are plotted in Figure 4a. The SF2 values for all cell cultures are shown in Figure 4b. The normal stromal and epithelial cultures were the most radiosensitive based on SF2 values, even though they had the lowest levels of IR-induced apoptosis at similar doses. Furthermore, the apoptotic kill response in the DU-145 and Rat-1 HO Myc cell lines was quite disparate, despite similar clonogenic survival (see Figure 2b,c). We observed that the DU-145 and PC-3 cell lines with altered p53 status were more radioresistant than the WTp53-expressing LNCaP cell line. However, defined experiments with prostate cell lines that are isogenic save for p53 status are required before concluding that p53 status correlates with radiosensitivity in prostate cancer cells. In summary, we have observed that the overall level of apoptosis was not correlated to the overall level of clonogenic cell survival in our panel of cell lines. Plotting the relative cell kill following 2 and 10 Gy based on the two endpoints in Figure 4c illustrates the discrepancy between the results of two assays.

Permanent arrest in irradiated prostate cells

Given that apoptosis was not a dominant mechanism for clonogenic cell kill, we next investigated the contribution of terminal growth arrest associated with senescence-associated markers to clonogenic survival using both a representative stromal culture (PrSC cells), and a representative epithelial culture (DU-145 cells). The choice of these two cultures was predicated on the need for cell lines which would readily form colonies following flow cytometric sorting procedures at 2 and 10 Gy and to

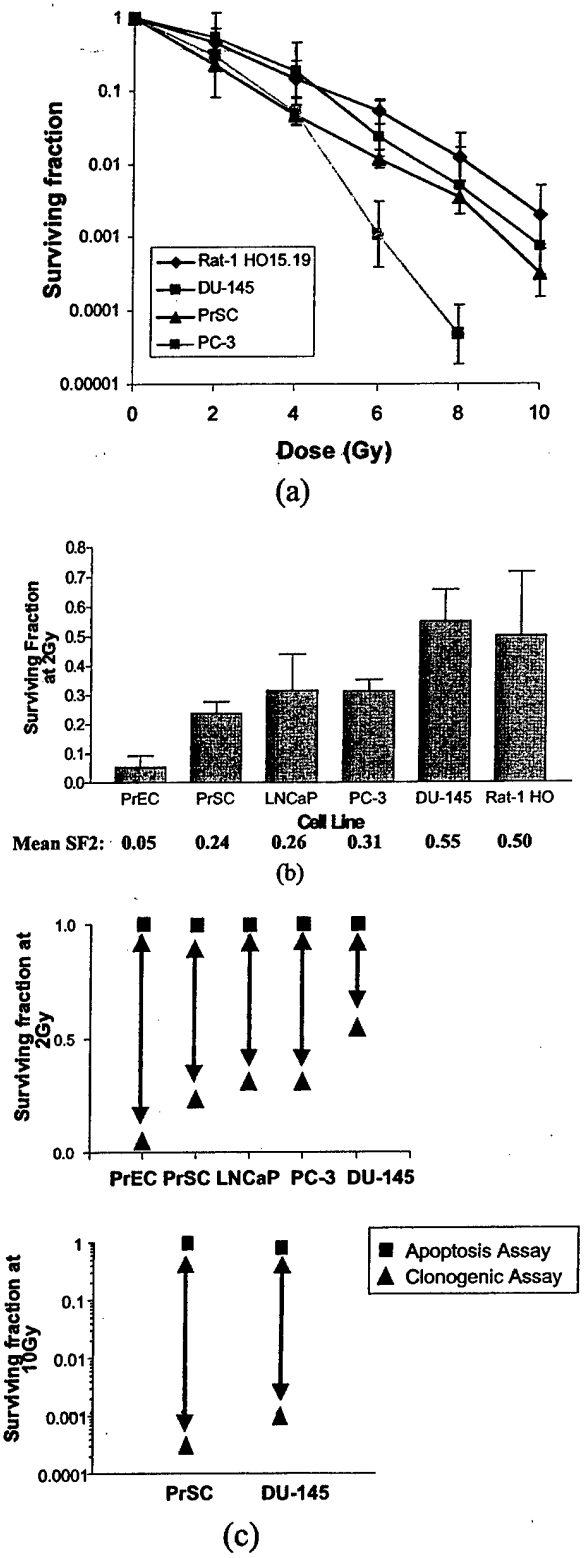

Figure 4 *Clonogenic survival data for normal and malignant prostate cultures: (a) full clonogenic radiation survival curves for PrSC, DU-145 and PC-3 and highly-apoptotic Rat-1 HO15.19 cell cultures (each point represents a geometric mean of three to five independent experiments plotted with associated geometric s.e.m.). (b) Surviving fraction following 2 Gy (SF2 values) with associated s.e.m. of normal and malignant prostate cell cultures. (c) Direct comparison of mean quantitative data for apoptotic and clonogenic kill following either 2 Gy (upper panel) or 10 Gy (lower panel).*

maximize the tissue-specific and genetic differences relating to propensity for senescence, clonogenic cell kill and G1 checkpoint control.

Using a flow cytometric assay that simultaneously determines relative levels of FL1-CFSE fluorescence (ie proliferation) and SSC-parameter (cell granularity), we determined that up to 87% of the PrSC population was non-proliferating with an associated increased granularity ($FL1(CFSE)^{hi}SSC^{hi}$) at 5 days, following a dose 10 Gy of radiation. In similarly plated cultures, only 14 and 8% showed the same cytometric profile in 2 Gy-treated or control cultures; these relative proportions being consistent over two or three representative experiments (Figure 5a, c). By comparison, only 32% of DU-145 cells had a senescent-like cytometric profile, although upon closer inspection the data suggest that the vast majority (ie greater than 70%) of DU-145 cells were actually non-proliferating, but that these cells were inconsistently associated with increased granularity when compared with stromal PrSC cells (compare CFSE-fluorescence axis in both cell lines following 10 Gy in Figure 5). The $FL1(CFSE)^{hi}SSC^{hi}$ cytometric profile was determined for 5% of DU-145 cells following 2 Gy and 3% in the untreated DU-145 population (Figure 5a, b; note that cells not growth-arrested following 2 Gy or in non-irradiated cultures may have undergone multiple rounds of division by this point differentially increasing the total 'proliferating' population). We then sorted and plated cells from the senescent-like, non-proliferating population relative to the remaining cells and observed that relative colony forming ability (plating efficiency) was decreased in the $FL1(CFSE)^{hi}SSC^{hi}$ ('non-proliferating'), SLP population in a dose-responsive manner (see Table 2).

In normal fibroblasts (ie stromal cells), cells undergo decreasing proliferative potential with increasing passage *in vitro*, until finally undergoing senescence associated with increased granularity, positive SA β-gal staining and upregulation of the $p21^{WAF1/Cip1}$ and $p16^{INK4a}$ proteins. Similar changes occur in normal fibroblast cultures when exposed to IR and has been referred to as a 'premature IR-induced senescence'.[40–42] Although we observed greater SA β-gal staining intensity in an increased number of PrSC stromal cells following a dose of 10 Gy (see Figure 6a), we found the endpoint to be highly variable across all cell lines and difficult to quantitate in epithelial cells (further data not shown; noted by others[43]). Whether upregulation of one or both genes is absolutely required for senescence and whether the process is p53-dependent in all cell types remains controversial.

In order to determine whether similar gene expression changes occurred in PrSC and DU-145 cells, we performed western blot analyses of cell populations obtained in parallel with flow cytometric experiments at day 5. These analyses showed high, IR-invariant levels of $p16^{INK4a}$ protein in both PrSC and DU-145 cultures and a dose-dependent increase in $p21^{WAF1/Cip1}$ levels in PrSC cells only (Figure 6b; confirmed using densitometry). We also analyzed $p16^{INK4a}$ expression in all of the cell cultures at 24 h following 10 Gy. In this case, levels of $p16^{INK4a}$ were either invariant (PrEC, LNCaP, DU-145) or undetectable (PrSC, PC-3) as confirmed by relative densitometry (data not shown). Long-term (up to 9 days) analysis of $p16^{INK4a}$ expression post-10 Gy irradiation DU-145 and PrSC demonstrated increasing

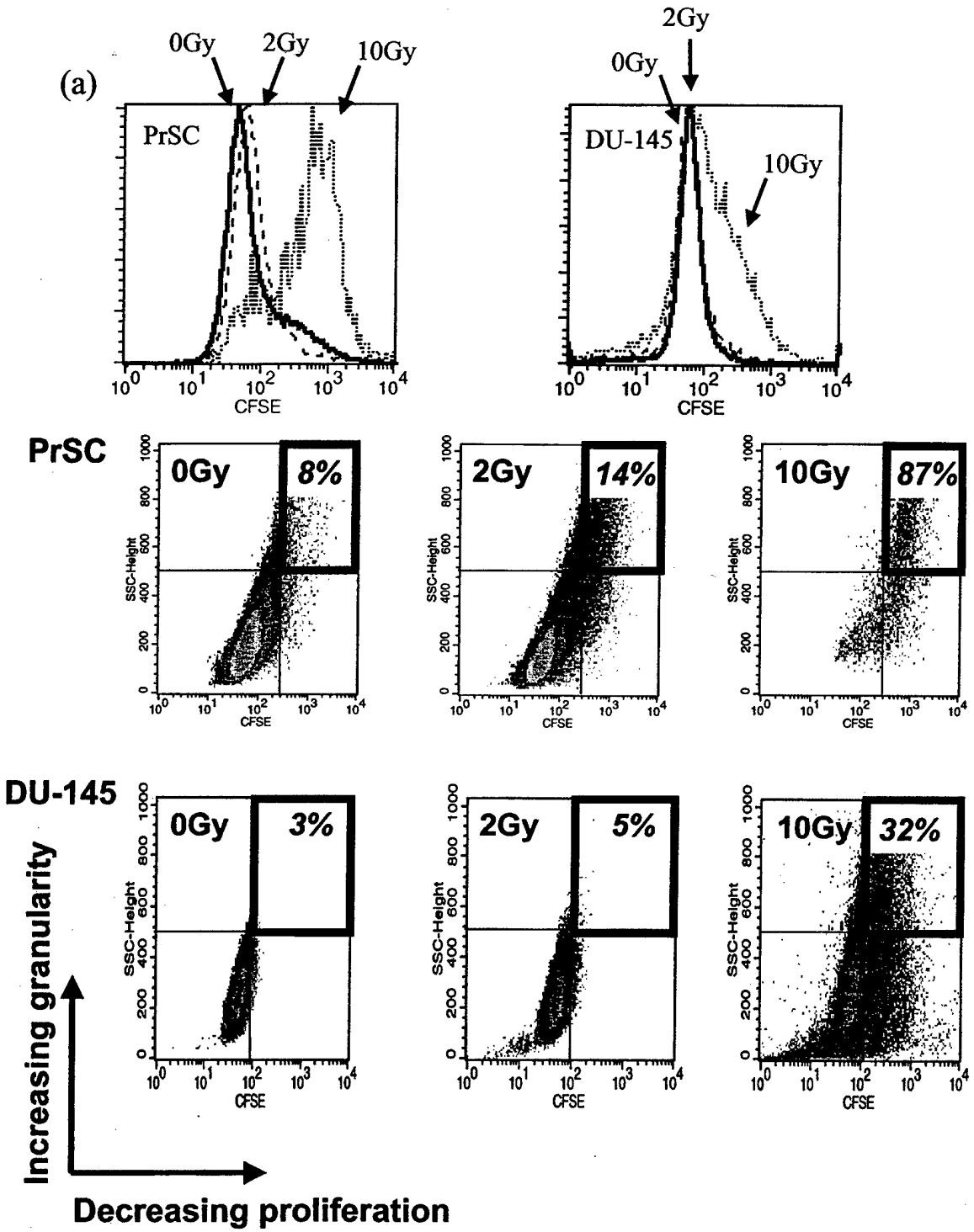

Figure 5 *Frequency histogram of FL1 fluorescence parameter (ie CFSE vital dye fluorescence) for (a) PrSC (left) and DU-145 (right) at 5 days post-irradiation following doses of 0 (control, mock-irradiated), 2 and 10 Gy. Shown is a representative experiment with total cell population analyzed for each dose. (b) Two-dimensional plots of FL1(CFSE) fluorescence intensity vs SSC (side scatter-granularity) for total cell numbers in mock irradiated and irradiated flasks of cells (see text for details) for PrSC (top) and DU-145 (bottom). Note increasing FL1(CFSE)^{hi} SSC^{hi} fractional sub-population (representing a senescent-like phenotype) with increasing dose; similar cytometric data was observed in all replicate experiments. These populations as shown were sorted using flow cytometry to determine relative colony forming ability as tabulated in Table 2.*

expression with time (data not shown), suggesting a time-dependent, though not dose-dependent, expression of p16^{INK4a}. We conclude that cells within a terminally arrested population that have increased cellular granularity (SLP) are incapable of forming colonies and that the sub-population of proliferating cells without associated increased granularity defines the colony-forming potential of the entire irradiated culture.

Table 2 Relative colony forming ability within FL1(CFSE)^{hi}SSC^{hi} (non-proliferating) and proliferating populations, as sorted by flow cytometry at day 5 post-irradiation

Cell type	Dose (Gy)	Number of cells plated	Plating efficiency (proliferating)	Plating efficiency (non-proliferating)
PrSC	0	100	0.33 ± 0.34[a]	0.03 ± 0.02
	2	1000	0.06 ± 0.03	0.01 ± 0.01
	10	1000	0.00 ± 0.00	0.00 ± 0.00
DU-145	0	100	0.41 ± 0.35	0.15 ± 0.14
	2	1000	0.22 ± 0.17	0.01 ± 0.01
	10	1000	0.01 ± 0.00	0.00 ± 0.00

[a]Mean values and associated s.e.m.

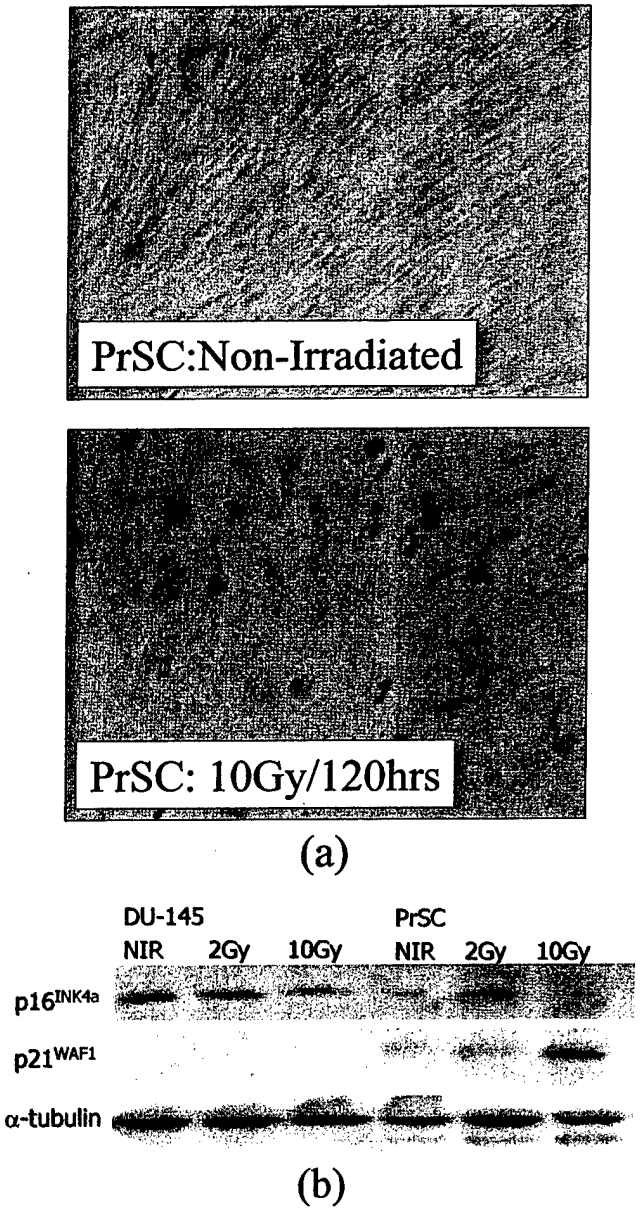

Figure 6 *Senescent biomarkers in prostate cell populations: (a) example of negative (left) and positive (right) SA β-gal staining in non-irradiated and irradiated PrSC cultures respectively, at 120 h following a dose of 10 Gy; (b) western blot analysis of p16^{INK4a} and p21$^{WAF1/Cip1}$ protein expression in entire PrSC and DU-145 cultures at day 5 following irradiation.*

Discussion

This is the first report, to our knowledge, documenting the relative role of apoptosis and terminal growth arrest as factors in determining overall clonogenic radiation cell survival for a panel of normal and malignant prostate cell cultures within the same laboratory setting. Using clinically relevant radiation doses, we observed a strong molecular apoptotic response in certain cell lines (bax and p53 upregulation in LNCaP cells, post-IR), yet this response did not correlate with quantitative determinations of apoptosis using morphology endpoints. The apoptotic response was not dose-responsive and did not correlate with final clonogenic cell kill. Further support for our data are the observations that manipulation of the ceramide-sphingomyelin and bcl-2-associated apoptotic pathways, or androgen ablation, can increase the apoptotic responses of prostate cells without altering final clonogenic radiation survival (K Shim and RG Bristow, unpublished observation[22,23,44]). Many groups have indicated that apoptosis may be the primary mode of death following gamma-irradiation only in specific cell types such as hematopoetic or lymphocytic cells, but not in stromal- or epithelial-derived tissues.[16,44–47] Furthermore, many attempts to alter apoptotic indices in epithelial- and stromal-derived tissues have failed to affect clonogenic survival. This suggests that, although the apoptotic pathway is intact in malignant prostate cells, other death mechanisms may override this response following irradiation.

It has been suggested that epithelial cell G1 checkpoint may be abrogated or less efficient than that of its stromal counterpart, despite wild-type p53 status. Girinski *et al*[36] found an abrogated p21$^{WAF1/Cip1}$ induction and G1 checkpoint in a panel of normal prostate epithelial cells as compared to a panel of normal prostate stromal cells following ionizing radiation. Meyer *et al*[48] reported similar findings for mammary epithelial *vs* stromal tissues. Within the same group, Romonov *et al*[49] observed an abrogated response to replicative crisis in the mammary epithelial cells suggesting a global defect in epithelial response to stress in comparison to its stromal counterpart. Our own experiments illustrated that, even for similar levels of p53 induction/stabilization, the p21$^{WAF1/Cip1}$ response in PrEC is greatly attenuated in comparison to its stromal counterpart. While the p53/p21$^{WAF1/Cip1}$ responses for our panel of malignant cell lines were as previously reported, the LNCaP cell line's

strong $p21^{WAF1/Cip1}$ induction is still surprising in light of its epithelial nature. Girinski *et al*[36] suggested that epithelial cell response might be partially dependant on interactions with surrounding stromal tissues.[37,50,51] LNCaP cells may have altered characteristics such that it does not require this interaction for a strong $p21^{WAF1/Cip1}$ induction following irradiation. Furthermore, studying G1 arrest alone may not be sufficient, since cells lacking a functional G1 checkpoint can exhibit a G2 delay that may be linked to DNA repair[52] and cellular survival following radiation.[53] Indeed, although our results suggest increased survival for cells which lack the G1 checkpoint, defined studies in isogenic tissue culture or solid tumor models which differ in p53 status and specific G1, S and G2 checkpoint control experiments are required to prove this hypothesis, and are part of a current research program.[11]

The success or failure of radical radiotherapy depends on the daily proportionate killing of tumor clonogens, which make up less than 1% of the total population of cells within a tumor. For example, it has been estimated that each gram of tumor contains approximately 1×10^9 tumor cells, with approximately less than 1×10^7 cells having clonogenic capacity. To date, no formal test or data exists for the pre-treatment determination of the number of clonogens existing prior to prostate radiotherapy. One can estimate that for a radiotherapy protocol using 35–40 fractions of 2 Gy, the clonogenic SF2 value should be less than 0.60 (ie death after 35 treatments $= 0.6^{35} = 1.7 \times 10^{-8}$) to cure a 1 g tumor, assuming equal killing per radiotherapy fraction.[4] Our data suggests that the SF2 *in vitro* is less than 0.6 for the cell lines tested. However, the effective SF2 may be higher *in vivo*, due to cell–cell interactions, hypoxia, altered gene expression or cell cycle phase during irradiation[3] and the relative importance of these factors remains to be determined in radiotherapy cohorts. Our observed *in vitro* radiosensitivity of normal epithelial and stromal cultures *in vitro* may explain the observation of glandular atrophy, fibrosis and decreased glandular function observed in prostate glands following irradiation. Exquisite sensitivity of normal epithelial cells may also explain why final post-therapy nadir PSA values in patients who achieve local control are lower than the PSA values in men without a diagnosis of prostate cancer, reflecting residual normal gland function after IR-induced cell kill.[54]

In our experiments, relative clonogenic cell kill was approximated by quantitative endpoints of a dose-responsive terminal growth arrest, in which certain cells acquired a senescent-like phenotype. Terminal growth arrest, rather than apoptosis, may begin to explain the slow kinetics of decreasing PSA values following radiotherapy over 12–16 months following treatment.[2] Recent experiments by Pollack and colleagues[23,55] are consistent with our data, as the supra-additive radioresponses observed in LNCaP and Dunning rat R3327-G tumor models following combined androgen withdrawal and fractionated radiation (mimicking clinical stage T3-T4 prostate cancer treatment protocols which increase overall patient survival).[56] were secondary to factors which determined post-treatment cellular growth arrest rather than apoptosis.

If a surrogate measure of radiation sensitivity was developed to use prior to, or early during, the course of radiotherapy, specific measures could be used to increase radiocurability or abort radiotherapy altogether in favor of radical prostatectomy (if medically feasible). Crook *et al*[57] found that markers of proliferation (PCNA, MIB-1) in post-radiotherapy biopsies from 498 men were an independent indicator of treatment failure, but indeterminate biopsies do occur which complicate interpretation as to whether viable clonogenic cells remain 2–2.5 y following radical radiotherapy. Our data suggests that other surrogate predictive factors might include molecular or cellular senescence or cell cycle arrest factors, such as the cdk inhibitors, $p21^{WAF}$ or $p16^{INK4a}$ that are activated by DNA damage and lead to altered proliferation and terminal growth arrest.

At present, no predictive test can determine which cells in the tumor are prostate clonogens rather than non-clonogens, however we believe that terminal growth arrest should be further investigated as a major mechanism of cell death in addition to apoptosis, in protocols that utilize radiotherapy. If proven to be important in prostate cancer, the former mechanism of cell death might be augmented *in vivo* using radiotherapy in conjunction with inhibitors of prostate cancer cell proliferation such as retinoic acid, antisense to cdk inhibitors, inhibitors of telomerase, or inhibitors of histone deactylase (HDAC).[58,59] Indeed these agents are currently being prospectively tested as single agents or in combination with chemotherapy in phase I/II trials; our results suggest further studies of the efficacy of these agents in combination with radiation as a novel prostate treatment strategy are necessary.

Acknowledgements

The authors would like to thank Dr L Chung for donating our LNCaP cell line, and Dr L Penn and E Soucie for the Rat-1 HO15.19 cell line. Special thanks to S Al Rashid, C Cantin, and F Jalali for help in selected assays and guidance. These studies were supported by the National Cancer Institute of Canada, the Princess Margaret Hospital Foundation and the US Army DOD Prostate Research Program.

References

1 Lukka H *et al*. Controversies in prostate cancer radiotherapy: consensus development. *Can J Urol* 2001; **8**: 1314–1322.
2 Dearnaley DP. Radiotherapy and combined modality approaches in localised prostate cancer. *Eur J Cancer* 2001; **37**: S137–145.
3 Bristow RG, Hill P. Molecular and cellular basis of radiotherapy In: Tannock IF and Hill RP (eds). *The Basic Science of Oncology*. McGraw-Hill: Toronto, 1998, pp 295–321.
4 Wong CS, Hill RP. Experimental Radiotherapy In: Tannock IF and Hill RP (eds). *The Basic Science of Oncology*, 3rd edn. McGraw-Hill: Toronto, 1998, pp 322–349.
5 Sandford NL, Searle JW, Kerr JF. Successive waves of apoptosis in the rat prostate alter repeated withdrawal of testosterone stimulation. *Pathology* 1984; **16**: 400–410.
6 Kyprianou N, Issacs JT. Expression of transforming growth factor-beta in rat ventral prostate during castration-induced programmed cell death. *Mol Endocrinol* 1989; **3**: 1515–1522.
7 Bruckheimer EM *et al*. The impact of bcl-2 expression and bax deficiency on prostate homeostasis *in vivo*. *Oncogene* 2000; **19**: 2404–2412.
8 Westin P, Stattin P, Darnber JE, Bergh A. Castration therapy rapidly induces apoptosis in a minority and decreases cell proliferation in a majority of human prostatic tumors. *Am J Pathol* 1995; **146**: 1368–1375.

9 Rakozy C *et al.* Expression of bcl-2, p53, and p21 in benign and malignant prostatic tissue before and after radiation therapy. *Mod Pathol* 1998; **11**: 892–899.
10 Grossfeld GD *et al.* Locally recurrent prostate tumors following either radiation therapy or radical prostatectomy have changes in Ki-67 labeling index, p53 and bcl-2 immunoreactivity. *J Urol* 1998; **159**: 1437–1443.
11 Bristow RG, Benchimol S, Hill RP. The p53 gene as a modifier of intrinsic radiosensitivity: implications for radiotherapy. *Radiother Oncol* 1996; **40**: 197–223.
12 Bristow RG, Benchimol S, Hill R. p53 protein expression or protein function? *Int J Radiat Oncol Biol Phys* 1996; **35**: 1123–1125.
13 Dewey WC, Ling CC, Meyn RE. Radiation-induced apoptosis: relevance to radiotherapy. *Int J Radiat Oncol Biol Phys* 1995; **33**: 781–796.
14 Olive PL, Vikse CM, Vanderbyl S. Increase in the fraction of necrotic, not apoptotic, cells in SiHa xenograft tumours shortly after irradiation. *Radiother Oncol* 1999; **50**: 113–119.
15 Stephens LC *et al.* Development of apoptosis in irradiated murine tumors as a function of time and dose. *Radiat Res* 1993; **135**: 75–80.
16 Tannock IF, Lee C. Evidence against apoptosis as a major mechanism for reproductive cell death following treatment of cell lines with anti-cancer drugs. *Br J Cancer* 2001; **84**: 100–105.
17 Schwarze SR *et al.* Role of cyclin-dependent kinase inhibitors in the growth arrest at senescence in human prostate epithelial and uroepithelial cells. *Oncogene* 2001; **20**: 8184–8192.
18 Stein GH, Drullinger LF, Soulard A, Dulic V. Differential roles for cyclin-dependent kinase inhibitors p21 and p16 in the mechanisms of senescence and differentiation in human fibroblasts. *Mol Cell Biol* 1999; **19**: 2109–2117.
19 Chang BD *et al.* A senescence-like phenotype distinguishes tumor cells that undergo terminal proliferation arrest after exposure to anticancer agents. *Cancer Res* 1999; **59**: 3761–3767.
20 Lyons AB, Hasbold J, Hodgkin PD. Flow cytometric analysis of cell division history using dilution of carboxyfluorescein diacetate succinimidyl ester, a stably integrated fluorescent probe. *Meth Cell Biol* 2001; **63**: 375–398.
21 Soucie EL *et al.* Myc protentiates apoptosis by stimulating Bax activity at the mitochondria. *Mol Cell Biol* 2001; **21**: 4725–4736.
22 Garzotto M *et al.* Reversal of radiation resistance in LNCaP cells by targeting apoptosis through ceramide synthase. *Cancer Res* 1999; **59**: 5194–5201.
23 Pollack A *et al.* Lack of prostate cancer radiosensitization by androgen deprivation. *Int J Radiat Oncol Biol Phys* 2001; **51**: 1002–1007.
24 Bristow RG *et al.* Radioresistant MTp53-expressing rat embryo cell transformants exhibit increased DNA-dsb rejoining during exposure to ionizing radiation. *Oncogene* 1998; **16**: 1789–1802.
25 Lee ST *et al.* Bcl-2 targeted to the endoplasmic reticulum can inhibit apoptosis induced by Myc but not etoposide in Rat-1 fibroblasts. *Oncogene* 1999; **18**: 3520–3528.
26 Kurts C *et al.* Class I-restricted cross-presentation of exogenous self-antigens leads to deletion of autoreactive CD8(+) T cells. *J Exp Med* 1997; **186**: 239–245.
27 Altieri DC. The molecular basis and potential role of survivin in cancer diagnosis and therapy. *Trends Mol Med* 2001; **7**: 542–547.
28 Ambrosini G, Adida C, Altieri DC. A novel anti-apoptosis gene, survivin, expressed in cancer and lymphoma. *Nat Med* 1997; **3**: 917–921.
29 Slingerland JM, Tannock IF. Cell proliferation and cell death In: Tannock IF, Hill RP. (eds). *The Basic Science of Oncology*, 3rd ed. McGraw-Hill: Toronto, 1998, pp 134–165.
30 Kaufmann SH *et al.* Specific proteolytic cleavage of poly(ADP-ribose) polymerase: an early marker of chemotherapy-induced apoptosis. *Cancer Res* 1993; **53**: 3976–3985.
31 Winter RN, Kramer A, Borkowski A, Kyprianou N. Loss of caspase-1 and caspase-3 protein expression in human prostate cancer. *Cancer Res* 2001; **61**: 1227–1232.
32 Olive PL. DNA damage and repair in individual cells: applications of the comet assay in radiobiology. *Int J Radiat Biol* 1999; **75**: 395–405.
33 Wahl GM, Carr AM. The evolution of diverse biological responses to DNA damage: insights from yeast and p53. *Nat Cell Biol* 2001; **3**: E277–286.
34 Giaccia AJ, Kastan MB. The complexity of p53 modulation: emerging patterns from divergent signals. *Genes Dev* 1998; **12**: 2973–2983.
35 Carroll AG, Voeller HJ, Sugars L, Gelmann EP. p53 oncogene mutations in three human prostate cancer cell lines. *Prostate* 1993; **23**: 123–134.
36 Girinsky T *et al.* Attenuated response of p53 and p21 in primary cultures of human prostatic epithelial cells exposed to DNA-damaging agents. *Cancer Res* 1995; **55**: 3726–3731.
37 Krtolica A *et al.* Senescent fibroblasts promote epithelial cell growth and tumorigenesis: a link between cancer and aging. *Proc Natl Acad Sci USA* 2001; **98**: 12072–12077.
38 Leith JT. *In vitro* radiation sensitivity of the LNCaP prostatic tumor cell line. *Prostate* 1994; **24**: 119–124.
39 DeWeese TL, Shipman JM, Dillehay LE, Nelson WG. Sensitivity of human prostatic carcinoma cell lines to low dose rate radiation exposure. *J Urol* 1998; **159**: 591–598.
40 Suzuki K *et al.* Radiation-induced senescence-like growth arrest requires TP53 function but not telomere shortening. *Radiat Res* 2001; **155**: 248–253.
41 Rave-Frank M *et al.* *In vitro* response of human dermal fibroblasts to X-irradiation: relationship between radiation-induced clonogenic cell death, chromosome aberrations and markers of proliferative senescence or differentiation. *Int J Radiat Biol* 2001; **77**: 1163–1174.
42 Kamijo T *et al.* Loss of the ARF tumor suppressor reverses premature replicative arrest but not radiation hypersensitivity arising from disabled atm function. *Cancer Res* 1999; **59**: 2464–2469.
43 Chang BD *et al.* Molecular determinants of terminal growth arrest induced in tumor cells by a chemotherapeutic agent. *Proc Natl Acad Sci USA* 2002; **99**: 389–394.
44 Kyprianou N, King ED, Bradbury D, Rhee JG. bcl-2 overexpression delays radiation-induced apoptosis without affecting the clonogenic survival of human prostate cancer cells. *Int J Cancer* 1997; **70**: 341–348.
45 Sheridan MT, West CM. Ability to undergo apoptosis does not correlate with the intrinsic radiosensitivity (SF2) of human cervix tumor cell lines. *Int J Radiat Oncol Biol Phys* 2001; **50**: 503–509.
46 Lock RB, Stribinskiene L. Dual modes of death induced by etoposide in human epithelial tumor cells allow Bcl-2 to inhibit apoptosis without affecting clonogenic survival. *Cancer Res* 1996; **56**: 4006–4012.
47 Aldridge DR, Arends MJ, Radford IR. Increasing the susceptibility of the rat 208F fibroblast cell line to radiation-induced apoptosis does not alter its clonogenic survival dose-response. *Br J Cancer* 1995; **71**: 571–577.
48 Meyer KM, Hess SM, Tlsty TD, Leadon SA. Human mammary epithelial cells exhibit a differential p53-mediated response following exposure to ionizing radiation or UV light. *Oncogene* 1999; **18**: 5795–5805.
49 Romanov SR *et al.* Normal human mammary epithelial cells spontaneously escape senescence and acquire genomic changes. *Nature* 2001; **409**: 633–637.
50 Kabalin JN, Peehl DM, Stamey TA. Clonal growth of human prostatic epithelial cells is stimulated by fibroblasts. *Prostate* 1989; **14**: 251–263.
51 Camps JL *et al.* Fibroblast-mediated acceleration of human epithelial tumor growth *in vivo*. *Proc Natl Acad Sci USA* 1990; **87**: 75–79.
52 Kao GD, McKenna WG, Yen TJ. Detection of repair activity during the DNA damage-induced G2 delay in human cancer cells. *Oncogene* 2001; **20**: 3486–3496.
53 Hwang A, Muschel RJ. Radiation and the G2 phase of the cell cycle. *Radiat Res* 1998; **150**: S52–59.
54 Gaudin PB *et al.* Histopathologic effects of three-dimensional conformal external beam radiation therapy on benign and malignant prostate tissues. *Am J Surg Pathol* 1999; **23**: 1021–1031.
55 Pollack A *et al.* The early supra-additive apoptotic response of R3327-G prostate tumors to androgen ablation and radiation is not sustained with multiple fractions. *Int J Radiat Oncol Biol Phys* 2000; **46**: 153–158.

56 Bolla, M *et al.* Improved survival in patients with locally advanced prostate cancer treated with radiotherapy and goserelin. *New Engl J Med* 1997; **337**: 295–300.
57 Crook J *et al.* Postradiotherapy prostate biopsies: what do they really mean? Results for 498 patients. *Int J Radiat Oncol Biol Phys* 2000; **48**: 355–367.
58 Suenaga M *et al.* Histone deacetylase inhibitors suppress telomerase reverse transcriptase mRNA expression in prostate cancer cells. *Int J Cancer* 2002; **97**: 621–625.
59 Marks PA, Rifkind RA, Richon VM, Breslow R. Inhibitors of histone deacetylase are potentially effective anticancer agents. *Clin Cancer Res* 2001; **7**: 759–760.

"Defective Rad51 Nuclear Translocation Following DNA Damage in Malignant Prostate Cells: Implications for Carcinogenesis and Therapy"

Fan R[4], Bromfield, G[3], Kumaravel, TS*[4], Sweet, J[2,5], Ozcelik, H.* and Bristow RG[1,3,4,5]

Departments of Radiation Oncology[1], Pathology[2] and Medical Biophysics[3], University of Toronto and Experimental Therapeutics Division[4], Ontario Cancer Institute and the Princess Margaret Hospital[5] (University Health Network), Toronto, Canada
*Samuel Luenfield Research Institute, Mount Sinai Hospital and University of Toronto.

*Present Address: Study Director Cytogenetics; Genetic and Molecular Toxicology
Covance Labs limited, Otley Road, Harrogate HG3 2XQ; United Kingdom

Key Words: prostate cancer, homologous recombination, Rad51, BRCA2, BRCA1, carcinogenesis

Running Title: *Rad51 and Prostate Cancer*

Correspondence to:

Robert G. Bristow, MD PhD FRCPC
Radiation Medicine Program
Princess Margaret Hospital (UHN)
610 University Avenue
Toronto, Ontario
CANADA M5G2M9
Fax: 416-946-4586
Phone: 416-946-2129
Email: rob.Bristow@rmp.uhn.on.ca

ABSTRACT

The Rad51 protein plays a pivotal role in gene conversion during homologous recombination induced by ionizing (IR) or ultraviolet (UV) irradiation, alkylating agents and replication elongation agents. Following DNA damage, the Rad51 protein translocates to the nucleus and forms distinct punctuate intranuclear foci at sites of recombinational DNA repair. Cells defective for Rad51-mediated homologous recombination (HR) show increased rates of mutagenesis and are predisposed to the malignant phenotype. In this study, we determined the expression of Rad51 mRNA and protein in both normal (PrEC-epithelial and PrSC-stromal) and malignant (LNCaP, DU-145 and PC-3; all epithelial) prostate cells, in relation to other genes and proteins involved in DNA-dsb repair. In all malignant prostate cell lines, the mRNA and protein levels of Rad51, XRCC3, Rad54 and variably, Rad52, mRNA were elevated ~4-5 fold, in comparison to normal prostate cultures. Ku70 mRNA and protein was also differentially elevated in the malignant cells. In contrast, we did not observe differential expression of Rad50, Mre11, Nbs1, Rad52, DNA-PKcs, Ku80, XRCC4 or LigaseIV. Using quantitative immuno-fluorescent confocal microscopy, we determined that the γH2AX response following IR (a biomarker of DNA-dsbs) was similar among the five cell lines tested. In contrast, we detected a decrease in the ability of Rad51 to form intranuclear foci following exposure to IR and MMC in the LNCaP, PC3 and DU-145 cells. This suggests that despite their high levels of Rad51 protein expression *in vitro*, malignant prostate cells may have decreased function of Rad51 associated with an inability to translocate to the cell nucleus and bind to sites of DNA damage. We show that this defect is associated with additional defects in BRCA1 and BRCA2 function in the LNCaP and PC3 cell lines. Following immunohistochemical staining for Rad51 in a series of human prostate xenografts and primary human prostate biopsies, we observed intratumoural heterogeneity of cellular Rad51 expression suggesting that epigenetic factors can further modify Rad51 expression *in vivo*. Our results suggest that the high levels of Rad51 protein observed in prostate cancer may have be dysfunctional based on altered nuclear trafficking, thereby implicating the Rad51-pathway as a possible determinant of genetic instability in prostate carcinogenesis.

INTRODUCTION

Tumor progression in a number of epithelial malignancies has been associated with the sequential loss of function of genes involved in cell cycle checkpoint control(*1*), DNA repair and cell death (ie apoptosis and terminal senescence)(*2,3*) which protect against DNA damage. For example, approximately 5% of breast cancer results from a genetic predisposition to the disease caused by mutations in the BRCA1 or BRCA2 tumor susceptibility proteins(*4-6*). These proteins act within the homologous recombination (HR) DNA repair pathway to repair DNA-double strand breaks (dsbs) which occur endogenously during cellular metabolism or following exposure to DNA damaging agents such as chemicals or ionizing (IR) and ultraviolet (UV) radiation(*7*).

In human cells, recombinational repair of DNA-dsbs occurs by homologous recombination (HR) and/or non-homologous recombination (ie. end-joining/NHEJ)(*8*). Direct end-joining (ie. NHEJ) requires little or no homology on the ends of the strands being joined, is more error-prone and predominates in somatic mammalian cells during the G1 and early S phases of the cell cycle(*9*). Two main discrete repair protein complexes are implicated in the end-joining pathway: (1) the DNA-PK/XRCC4/LigIV complex and (2), the MRE11/RAD50 complex. In homologous recombination, extensive homology is required between the region of the DNA-dsb, and the sister chromatid or homologous chromosome from which repair is directed and involves the Rad51, Rad52, Rad54, Rad55-57 and RPA proteins. The HR pathway is thought to predominate in germline tissues in the late S/G2 phases of the cell cycle and provides error-free repair(*9-12*).

Rad51 is a structural, and functional, eukaryotic homologue of the E. coli RecA recombinase and forms nucleoprotein filaments on ssDNA mediating homologous paring and strand exchange reactions between ssDNA and homologous double-stranded DNA(*10*). Rad51 has a number of paralogues including the XRCC2, XRCC3 and Rad51B/C/D proteins and function as part of a larger recombination complex that includes Rad52, Rad54 and RPA(*13-16*). Current models suggest that Rad51 is a stably-associated core component of the multi-protein HR-repair complex at sites of DNA damage and that its associated proteins, Rad52 and Rad54, rapidly and reversibly interact with the focal Rad51 complex(*17*). The Rad51 protein therefore plays a pivotal role in gene conversion during homologous recombination induced by ionizing (IR) or ultraviolet (UV) irradiation, alkylating agents, and replication elongation agents and is involved in sister-chromatid exchange (SCE)(*18-20*). Cells defective for Rad51-mediated recombination show increased rates of mutagenesis and chromosomal rearrangements and attempts at generating a murine rad51-knockout animal have failed given embryonic lethality(*21-23*).

Immunofluorescent confocal microscopy studies(*24*) support that cytoplasmic Rad51 can translocate to the nucleus as intranuclear foci following irradiation and co-localize with RPA at sites of unscheduled DNA synthesis and recombinational repair(*25*). This is similar to the rapid appearance of the γ-H2AX histone phosphoform which has been shown to be a quantitiative marker for DNA-double strand breaks (dsbs) and co-localize with the BP53-1, BRCA1, Rad50 and Rad51 proteins at DNA breaks in a sequential and temporal manner(*26,27*). By 24 hours post-irradiation, most Rad51 nuclear foci are sequestered into micronuclei or assembled onto Rad51-coated DNA fibers that display genome fragmentation typical of apoptotic death(*28*). Importantly, the level of RAD51 irradiation-induced foci (IRIF) relate to the capacity for genetic recombination such that the level of Rad51 IRIF is a direct reflection of the baseline or IR-induced frequency of homologous recombination within cells(*29*) (SN.Powell-MGH-submitted, 2002 and personal communication). The relative capacity for HR among various cell lines can also be determined using plasmid assays which measure inter-chromosomal gene

conversion; by determining the relative level of SCEs; and by the relative sensitivity to cross-linking agents such as MMC.

Data is rapidly associating the function of Rad51 itself or its association with HR-related proteins BRCA1, BRCA2, RAD54 and XRCC2/3 to the development of breast, prostate, ovarian, pancreatic and thyroid cancer(*13,30-36*). More recently, the BRCA1 and BRCA2 cancer-susceptibility proteins have been suggested to play a role in the homologous repair of DNA-dsbs through direct interaction with Rad50 and Rad51, respectively(*37-40*). BRCA2 is a large protein which contains a cluster of eight BRC repeats encoded by exon 11 in which the more highly conserved BRC repeats (ie BRC1-4, BRC7 and BRC8) are interactive domains with the Rad51 protein(*41-43*). Additionally, in the mouse, a further interaction between these two proteins occurs through a motif in the carboxyl terminus of BRCA2. Interactions between BRC3 and BRC4 regions of BRCA2 block nucleoprotein filament formation by Rad51 on the 3' end of DNA breaks. In BRCA2-defective (eg. the Capan-1 pancreatic cell line which expresses a truncated BRCA2 protein or $BRCA2^{-/-}$ murine cells) and BRCA1-defective cells, Rad51 fails to localize to the nucleus in response to genotoxic stress(*37,44*). Therefore BRCA2 regulates both the DNA binding ability of Rad51 and localization to the nucleus following DNA damage(*45*). Rad51 can also functionally interact with other cell cycle checkpoint and oncogenic proteins such as p53, ATM, BRCA1, c-abl, bcl-2 and BLM which altogether, strongly supports Rad51 pathways as a determinant of cellular carcinogenesis(*1,46-52*).

There are increasing reports of elevated levels of Rad51 mRNA and protein expression occurring *de novo* within human tumours(*53,54*). Both DNA microarray and protein expression data suggest Rad51 protein levels are elevated in pancreatic cancer, a cancer that is uniformly chemoresistant and radioresistant(*53,55*). This data is supported by certain Rad51 over-expression studies in which increased $p21^{WAF}$ expression and a decreased apoptotic response were both correlated to radioresistance, *in vitro*. Overexpression of Rad51 has also been linked to increased resistance to chlorambucil, nitrogen mustard, caffeine, MMS, cisplatinum and mitomycin C(*37,42,56-58*). Increased Rad51 expression may therefore be advantageous to cancer cells if it leads to protection from DNA damage and apoptosis and also drives genetic instability towards aggressive tumour cell phenotypes(*21,59*).

It remains unknown whether the high levels of Rad51 expression observed in malignant cells *de novo* is directly correlated to an altered capacity for homologous recombination(*59-62*). In order to further study the association with altered Rad51 expression the malignancy, we determined the expression of Rad51 at the mRNA and protein levels in both normal (PrEC-epithelial and PrSC-stromal) and malignant (LNCaP, DU-145 and PC-3) prostate cells in relation to other DNA-dsb repair proteins. We report elevated expression of Rad51 and its associated repair complex members (XRCC3, Rad54 and variably, Rad52) in all three malignant prostate cell lines. Using baseline and IR-induced Rad51 intranuclear foci formation (ie IRIF formation) as a marker of homologous recombination, we observed defects in Rad51 nuclear translocation and HR-associated focus formation, despite the high expression of Rad51 in the malignant cell lines. This suggests that, despite high total cellular levels of Rad51 protein expression, Rad51 may be incapable of supporting unscheduled DNA synthesis and recombination following DNA damage due to a cytoplasmic to nuclear trafficking defect. Indeed, severe defects in Rad51 IRIF formation was associated with altered BRCA2 and/or BRCA1 function in selected cell lines. We discuss our findings in terms of prostate carcinogenesis and cellular resistance to cancer chemotherapy and radiotherapy.

RESULTS:

Increased gene expression of Rad51 complex genes in malignant prostate cancer

To initially verify the results of ribonuclease protection assays (RPA) in quantifying gene expression in our panel of 2 normal (PrEC-epithelial and PrSC-stromal) and 3 malignant (LNCAP, PC3 and DU-145; all epithelial) prostate cell lines, we first quantitated the radiation-induction of genes associated with the ATM/p53 cell cycle checkpoint pathway. We have previously reported (*Bromfield et al. In press, Prostate Cancer and Prostatic Associated Diseases, Dec., 2002*) the characteristics of these cell lines following IR and the results of p53 DNA sequencing studies (full length sequencing of exons 2-11). PrSC, PrEC and LNCaP cells express two wild type p53 alleles and have an intact G1 cell cycle arrest checkpoint and $p21^{WAF}$ expression following exposure to ionizing radiation (IR). PC-3 cells were devoid of p53 protein expression due to chromosome 17p hemizygosity and a mutation in the remaining allele at codon 138 that results in a premature stop codon at position 169. DU-145 cells express high levels of trans-dominant, mutant (MT) p53 proteins due to missense mutations at codons 223 and 274. Both these latter cell lines lack a G1 checkpoint and do not upregulate $p21^{WAF}$ following IR. All 5 cell cultures undergo minimal and non-differential apoptosis (<5%) after doses of up to 20 Gy (measured 12-96 hours post-IR), but the WTp53-expressing cell lines do induce bax protein, post-IR. The major mode of cell death is IR-terminal growth arrest (ie. cellular senescence) which is correlated to a long-term elevation of $p16^{INK4a}$ protein and relative surviving fraction for a given IR dose based on long-term clonogenic radiation survival data. The three malignant cell lines had the highest survival (ie mean SF2Gy values ranging from 0.4- 0.55 relative to the values for PrSC and PrEC, at 0.25 and 0.1, respectively).

Following irradiation with 10Gy, at 4 hours we observed increased expression of p21WAF, gadd45, bax and bcl-2 in the WTp53-expressing cells (ie. PrSC, PrEC and LNCaP), whereas similar increases in gene expression were not observed for the null-p53 and MTp53-expressing, PC3 and DU-145 cells (see Figure 1a and 1b). As previously observed (*Bromfield et al; In press*), the relative upregulation of $p21^{WAF}$ in PrEC epithelial cells was attenuated in comparison to PrSC stromal cells for a given IR dose. Neither ATM, nor p53, mRNA was increased following irradiation, consistent with previous data and data showing that p53 function is determined by post-translational modifications leading to stabilization following DNA damage, rather than rather than altered transcription. Furthermore, the level of PC3 (null-p53) p53 mRNA was at background. We confirmed relative $p21^{WAF}$ expression among the cell lines pre- and post-IR at the protein level using Western blot analyses based on lysates from parallel-irradiated cultures (data not shown). Furthermore, we confirmed a dose- and time-dependent (maximal induction at 4-6 hours post-IR) induction of $p21^{WAF}$ in the LNCaP cell line using RPA assays (data not shown) which confirmed previous Western blot analyses.

The initial data relating to ATM/p53 stress response provided confidence in the further use of RPA assays for quantification of gene expression relating to the non-homologous and homologous recombination pathways of DNA-dsb repair. The data in Figure 2 are consistent with an increased basal expression of the Ku70, Ku80 and DNA-PKcs genes in relation to the XRCC4 and Ligase IV genes. Not one of these genes was up-regulated at 4 hours following irradiation. Of the NHEJ genes, only Ku70 was differentially expressed at a higher level (both mRNA and protein-see insert lower panel) in malignant cells than the normal cells. In contrast, we observed a significant and differential increase (~2-3 fold) in Rad51-complex associated genes (ie. Rad51, Rad54, XRCC3 and variably, Rad52)(*13*) in malignant prostate cell cultures in comparison to normal cultures and this relative gene expression was not increased following irradiation (Figure 3a)(*63*). Genes relating to the Rad50-repair complex (ie Rad50, Mre11, Nbs1) were not differentially expressed among malignant and normal prostate cells. The increased expression of XRCC3 and Rad51 (~4 fold) were confirmed at the protein level using the

Western blot analysis presented in Figure 3b. We conclude that the expression of Rad51 and XRCC3 are increased at both the transcriptional, and translational, level in malignant prostate cell lines.

Defective Rad51 IRIF Responses in Malignant Prostate Cell Lines

Recent advances in immunofluorescent biology and confocal microscopy have afforded the visualization of DNA repair complexes at sites of DNA damage with cells *in situ*. The prototype of these ionizing radiation-induced intranuclear foci (IRIF) are the tri-protein Rad50-repair complex whose protein members (Rad50, Mre11 and Nbs1-nibrin) are translocated to the nucleus and form discrete punctate foci within areas of intranuclear DNA damage(*27*). More recently, the γ-H2AX histone phosphoform has been shown to be a specific and quantitiative protein for sites of DNA-double strand breaks (dsbs) and can co-localize with the BP53-1, BRCA1, Rad50/Mre11 and Rad51 proteins at DNA breaks in a sequential and temporal manner(*27*). In order to test the ability for malignant and normal prostate cells to form IRIF, we determined the relative qualitative and quantitative formation of γ-H2AX IRIF in all cell lines at 4 hours following 10 Gy. In all 5 cell lines and the Capan-1 pancreatic cell line which is BRCA2-defective, intranuclear γ-H2AX IRIF formation was observed to increase normally within 50-80% of cells having greater than 2 foci following irradiation and with similar numbers of γ-H2AX IRIF per nucleus among the cell lines (see Figure 4). To confirm the specificity of our antibody to γ-H2AX IRIF, we were able to show co-localization of this protein with Mre11, a member of the Rad50 repair complex. We also confirmed specificity of our anti-Rad51 antibody in that the Rad51-IRIF detected with this antibody co-localized as expected with RPA IRIF following irradiation (se Figure 5a).

Given the increased expression of Rad51 protein within our malignant cell lines and previous reports of increased Rad51-IRIF in malignant cells, we determined the level of Rad51-IRIF in our cell panel pre-and post irradiation. Both normal prostate cultures and a human fibroblast control showed evidence of increased quantity and size of Rad51 IRIF following irradiation (see Figure5b), although the cytoplasmic staining of Rad51 was increased in the PrEC culture pre- and post-IR. In contrast, in two of the three (ie. LNCaP and PC3) malignant prostate cell lines had grossly defective Rad51 IRIF responses following irradiation which were similar to the response of the negative Rad51 IRIF control cell line, Capan-1. Similar to PrEC cells, the cytoplasmic staining of Rad51 in the epithelial cell lines was greater than that observed for the stromal cell lines in Figure 5b and other Rda51staining data in a number of human fibroblast strains in our laboratory (*Jalali et al., Manuscript in preparation*). We further confirmed that the lack of Rad51 IRIF formation in the LNCaP cell line was both dose- and time-independent as in Figure 5d. The quantitative defect in Rad51 IRIF formation in the malignant prostate cell lines based on the number of Rad51 IRIF per nucleus or number of Rad51-IRIF positive cells is shown in Figure 6. Similar defects were observed for MMC-treated LNCaP and PC3 cells (data not shown). Despite expressing 3 to 5 fold excess cellular Rad51 protein (based on Western blot data), the Rad51-IRIF response in the malignant prostate cell line was attenuated. This suggests a defect in Rad51 cytoplasmic to nuclear trafficking (being confirmed with Western blotting of fractionated cytoplasmic and nuclear lysates), an altered ability of Rad51 to bind to DNA breaks within a repair complex or other Rad51-associated defects in these cells. If we assume that Rad51 IRIF are correlated with the capacity for homologous recombinational repair following DNA damage, our results suggest that the LNCaP and PC3 cell lines are deficient in this respect(*60*). Unfortunately, the use of HR plasmid-based, inter-chromosomal gene conversion assays to confirm this observation is difficult given the probable poor transfection efficiency of the PrSC and PrEC cells which is initially required in these assays to integrate recombination reporter substrates(*45*).

As BRCA2 and BRCA1 function may affect Rad51 translocation, we qualitatively determined whether BRCA2 translocation was altered in the Rad51-defective LNCaP and PC3 cells. Using Capan-1 cells as a negative control, we determined that PC3 and LNCaP have defective BRCA2 IRIF

formation (Figure 7a)(*64,65*) and possibly also BRCA1 IRIF defects (Figure 7b)(*31,66*). Recent work has shown that there one no Rad51, BRCA1 nor BRCA2 mutations may have 5 cell lines. Therefore, our results would suggest there must be alternate explanations for the defective Rad51 IRIF formation in our prostate cancer cell lines perhaps related to intracellular trafficking.

Heterogeneity of Rad51 Expression Within Prostate Cancer Xenografts and Primary Biopsies (studies are ongoing to test this hypothesis).

Given the increase Rad51 expression observed in vitro, we were curious to see whether a similar increase is observed in vivo when certain of the malignant cell lines form tumors as xenografts within immune-compromised mice. In PC3 xenografts, we observed heterogeneity of Rad51 staining within xenograft histologic sections with both cytoplasmic and nuclear staining patterns (Figure 8a). However, following irradiation in vivo with a single dose of 20 Gy, we observed increased and intensified Rad51 staining within the xenograft, however the resolution of microscopy and staining did not permit us to comment on actual Rad51 IRIF. Nonetheless, even after irradiation, there is great heterogeneity within the PC3 xenograft for Rad51 staining suggesting epigenetic actors may be operational *in vivo* to further modify Rad51 expression. Similar intratumoural heterogeneity was observed for Rad51 expression within primary biopsies of human prostate cancer (Figure 8b)

DISCUSSION

This is the first study to report altered nuclear translocation of the Rad51 protein as IRIF following DNA damage in malignant prostate cells. Radershall and colleagues (2001) reported increased percentages of Rad51 IRIF-positive cells in malignant cell lines when compared to normal cell lines or cultures, but we did not observe this simple relationship in our cell panel. This may be due to differences in antibody specificity or techniques of microscopy or IRIF formation. However our control antibodies and labeling conditions did not reveal high levels of background IRIF and we have successfully co-localized DNA repair protein complexes (ie Mre11/γH2AX and Rad51-RPA)(*27*) with our antibodies, as predicted from previous work. Instead we believe that by quantitating the IRIF formation per nucleus, both prior to, and following DNA damage, we are gathering complete data as to whether the increased expression of Rad51 protein as documented for malignant cells is indeed functional, based on IRIF formation data.

Our study also supports that functional BRCA2 protein is required for efficient translocation of Rad51 protein to the nucleus but awaits formal DNA sequencing of rad51, brca1 and brca2 genes in our cell lines which is currently underway(*65*). Alternatively, other proteins can interact with the Rad51 protein including the p53 protein (which inhibits Rad51-mediated HR), c-abl (which may be involved in Rad51 translocation) and bcl-2 (involved in post-translational phosphorylation of Rad51)(*50,67*). We thin it unlikely that our results are due to interactions with the p53 protein given the disparate Rad51 IRIF formation and p53 genotype between LNCaP, DU-145 and PC3 cell lines. It is of interest that both c-abl and bcl-2 can be located and function within the extranuclear endoplasmic reticulum (ER). On detailed microscopic analysis the ER is an area of the cytoplasm in which the Rad51 protein tends to accumulate following irradiation (ie contrast perinuclear clearing of rad51 staining in PrEC cells with increased perinuclear Rad51 staining in LNcaP and PC3 cells, post-irradiation, in Figures 5b and 5c). Immunofluorescent studies are ongoing which are attempting to co-localize Rad51 with selected cytoplasmic domains (ER, Golgi complexes, mitochondria and cytoplasmic vacuoles) as little work has been done in the area of intracellular Rad51 trafficking(*68*).

Epigenetic mechanisms may also affect Rad51 expression as Rad51 protein levels are increased to a greater extent in pancreatic cells when grown as xenografts rather than grown in tissue culture(*53*). This may explain the relative radio-and chemo-resistance of pancreatic cancer in which high levels of Rad51 can be further augmented by issues pertaining to the 3-D tumour microenvironment. Our own

data supports increased heterogeneity in prostate cancer xenografts, but also support an increase in expression following irradiation *in vivo*. Further experiments with defined doses and timepoints post-IR in LNCaP, PC3 and DU-145 cells (which have variable IRIF responses in vitro) growing as xenografts, may clarify these issues and glean more information regarding Rad51 expression within solid tumours(*53*). As yet, it is not understood whether the heterogenous staining pattern of Rad51 expression within tumours in vivo is secondary to cell cycle phase specificity, oxygenation or nutritional status or clonal variation among tumour cells. However, preliminary *in vitro* data from this laboratory suggest that Rad51 protein expression can be decreased by exposure to hypoxia (Coleman and Bristow, unpublished, 2002).

Our results implicate DNA repair, and particularly, homologous recombination, as a potential factor in prostate carcinogenesis and cancer therapy(*13,56*). Whether the IRIF defect observed for Rad51 is a direct determinant of carcinogenesis or is an indirect effect of genetic instability and the transformation process due to other gene mutations(*69,70*), requires defined isogenic models of prostate carcinogenesis in order to test this hypothesis. Our results also have implications for both prostate cancer diagnosis and therapy as we would hypothesize that prostate intraepithelial neoplasia (PIN) may have altered frequencies of homologous recombination and defective DNA-dsb repair when compared to nonmalignant epithelium. If true, there may be a role for Rad51 protein detection within core biopsies of patient cohorts within surveillance programs who are at high risk for prostate cancer based on abnormal PSA levels or strong family histories. Finally, given the correlation with high Rad51 expression and cancer therapy resistance in vitro, our study also supports the pre-clinical testing of anti-Rad51 cancer *treatments in vivo* based on the initial positive reports of radiosensitization with Rad51-antisense(*71,72*).

MATERIALS AND METHODS

Normal and Malignant Prostate Cell Culture and Characteristics

All cell cultures were incubated in vented tissue culture flasks under 5% CO_2 and 37°C culture conditions. LNCaP cells (a gift from L. Chung, University of Virginia) were maintained in T-media (Gibco-BRL) and supplemented with 10% FCS. PC-3 and DU-145 cells were purchased from ATCC and maintained as suggested in Ham's F12K, and alpha-Modified Eagles Medium respectively, supplemented with 10% FCS and 2mM L-glutamine. PrEC (normal prostate epithelial cells) and PrSC (normal prostate stromal cells) were purchased from Clonetics and maintained per suggested protocols: (1) prostate epithelial growth medium (PrEGM) contains BPE, insulin, Hydrocortisone, GA-1000, retinoic acid, transferrin, epinephrine, hEGF, triiodothyronine and (2) stromal cell growth medium (SCGM) includes hFGF-B, insulin, FBS and GA-1000 medium (Clonetics Inc, San Diego, CA). All cell cultures and lines were maintained at 37^0C in a 5% CO_2 atmosphere without testosterone supplementation. Both cell cultures have limited lifespan and proliferative potential in culture according to the supplier and we have consistently observed decreased growth rates following passage 5 *in vitro* for both PREC and PRSC cultures. Approximate doubling times for cell cultures under these conditions were as follows: PrEC: 36-48 hours (highly variable), PrSC: 18 hours, LNCaP: 36 hours, PC-3: 24 hours and DU-145: 18 hours. The human pancreatic cell line, CAPAN-1, was used as a negative control for BRCA2 and Rad51 function as it contains a truncated form of BRCA2 (known as BRCA2 617delT) which is non-functional for Rad51-BRCA2 interactions and does not support BRCA2 or Rad51 protein translocation to the nucleus following DNA damage. This line was cultured in RPMI-1640 media supplemented with 10% FCS.

Conditions of Cellular Exposure to DNA Damaging Agents

Logarithmically growing cells were rinsed with PBS/HBSS, trypsinized for 5 minutes at 37°C, and then were seeded at appropriate densities in 6 or 10 mm dishes prior to RNA or protein extraction.

Asynchronous cultures were irradiated 16-20 hours post-plating to reduce the immediate effects of trypsinization and such that the multiplicity index was less that 1.1 (*73*). Plated cells were either mock irradiated or irradiated with 0 to 10Gy under aerobic conditions using a ^{137}Cs irradiator at ~ 1Gy/min at room temperature. For studies pertaining to DNA repair complex formation, (ie IRIF), prostate cells were seeded at a density of $5x10^4$-$1x10^5$ cells/ml in Permanox slides (chamber slides) and allowed to adhere for 16-36 hours for each experiment and irradiated as above with doses between 2-10 Gy. MMC was prepared as a stock solution of 0.5 mg/ml in distilled water; cells were then treated with MMC with 4.8ug/ml for 1 hour in tissue culture and then prepared for IRIF studies (see below) at 4 hours after MMC-addition.

Quantitative Expression (Pre- and Post-Irradiation) of Genes Associated With ATM/p53-mediated Cell Cycle Checkpoint Control and the Homologous and Non-Homologous Recombination Pathways of DNA-dsb Repair: Ribonuclease Protection Assays (RPA)

Asynchronously growing cells were harvested at 70-80% growth confluence from either non-irradiated cultures or 4 hours following a totals dose of 10Gy. Total RNA extracts for RPA analyses was isolated using Trizol reagent (Sigma Inc.) according to protocols provided by manufacturer. Twelve antisense riboprobes (RAD50, MRE11, RAD52, RAD54, RAD51, XRCC2, XRCC3, RAD51B, RAD51C, RAD51D, L32 and GAPDH) were synthesized with the RoboQuant multi-probe template sets (DBSR1, PharMingen Inc.), Twelve antisense riboprobes (ATM, NBS1, XRCC2, XRCC3, XRCC9, Ligase IV, XRCC4, Ku70, DNA-PK, Ku86, L32, GAPDH) were synthesized with the RoboQuant multi-probe template sets (DBSR2, PharMingen Inc.), another ten antisense riboprobes (Bcl-x, p53, Gadd45, c-fos, p21, Bax, Bcl-2, Mcl-1, L32, GAPDH) were synthesized with the RoboQuant multi-probe template sets (hstress, PharMingen Inc.), and purified by using the RPA MAXIscript method (Ambion Inc.). RPA was carried out using a modified procedure of the RPAIII (Ambion Inc.). 5ug of sample RNA was hybridized with 2000cpm of the synthesized multi-riboprobe in a single tube with 10 ml hybridization buffer, heated at 95C°for 5min, and then incubated at 56C° overnight. The hybridized RNA sample was digested with 20ng RNase A and 60U RNase T1 in 100ml of RNase buffer (RPA III, Ambion Inc.) by incubation at 30C° for 45min. The resultant sample was incubated with RPA inactivation/precipitation III solution at –80C° for 30min. A blue pellet was obtained by centrifuging at 10,000 rpm for 15min at 4C° and then washed with 70% ethanol. The final RNA pellet was air-dried, resuspended in 4ul loading buffer, denatured at 95C° for 5min, and kept on ice. The protected RNA sample was electrophoresed through a 6% acrylamide gel with 8M urea at 1200-1500Vt for 1-2hr. The sample gel was mounted on a 3MM paper and dried at 80C° for 1hr. The cpm value of the individual band on the gel was counted by Phosphor Imager (Storm 840, Molecular Dynamic Co.). The statement level of the GAPDH gene was used as an internal control. The relative statement levels of other individual genes were calculated as a ratio (i.e. the observed total volume for the target gene divided by the volume of GAPDH). Three different total RNA extracts were analyzed in triplicate for each cell line. The results of the three separate experiments are expressed as the mean value +/- 1 S.E.

Western blot Analyses for Relative Expression of HR and NHEJ Proteins

Logarithmically-growing cells were irradiated and lysed on ice for 20 minutes with E7 lysis buffer as previously described (*73*). The cells were homogenized at 4C° in E7 buffer (i.e., PBS, 0.1%SDS, containing protease inhibitors; Roche Molecular Biochemicals. Indianapolis, IN). The cell debris was pelleted by centrifugation at 12000g for 10 minute at 4C°, and the supernatants containing the protein extracts were frozen at –70C °until analysis. Protein quantification was performed determined using a commercial Pierce-BCA assay kit to derive a mean concentration value based on three assays per lysate. SDS-PAGE was performed using 7-12% bis-acrylamide (29:1) gels with a 4% stacking gel run in a Novex X-cell semi-dry Mini Cell western blotting apparatus at room temperature.

Each well was loaded with 20*ug* of total protein plus loading buffer (final concentration 1x-6% glycerol, 0.83% b-mercaptoethanol, 1.71% Tris-HCl pH 6.8, 0.002% Bromophenol Blue) after boiling for 3 minutes. Samples resolved by electrophoresis at 80-110 Volts for 1.5-2.5 hrs were transferred onto nitrocellulose (Schleicher&Schuell, Inc.), overnight at 14v/4°C or for 1.5 hours at 24v/room temperature in transfer buffer (75mM glycine, 10mM Tris, 20% methanol). For selected blots, pre-hybridization staining with Ponceau S confirmed equal loading and transfer between running lanes. To detect protein, membranes were blocked in 10% nonfat milk in PBS containing 0.2% Tween 20 (TBST) at room temperature for 2 hours and incubated with the primary antibody diluted in blocking solution for a further 2 hours at room temperature. Membranes were then rinsed with TBST and exposed to the appropriate secondary antibody for 1 hour under similar conditions, rinsed again with TBST, once with 10x TBS and finally incubated in Amersham ECL chemi-luminescence solution for one minute. Membranes were exposed to Hyperfilm ECL from AmershamPharmacia and analyzed by densitometry (Molecular Dynamics Computing Densitometer, ImageQuant Mac v.1.2) normalized against α–tubulin levels. Primary antibodies used in these studies at dilutions ranging from 1:200 to 1:1000 included: Rad51 (1:1000; Ab-1; Oncogene Research Products, Inc.), Rad50 (1:1000; NB100-147; Novus Biologicals, Inc), Rad52 (1:200; SC-8350; Santa Cruz Biotechnology Inc.), XRCC3 (1:1000; NB100-165; Novus Biologicals, Inc), p21 (1:500; OP64; Ab-1; Oncogene Research Products, Inc.), Ku70 (1:500; SC-1486; Santa Cruz), and α –tubulin (1:2000; CP06; Oncogene Research Products, Inc.).

Preparation of Cells for Detection of Intranuclear Foci of DNA repair proteins

At defined times after IR or MMC-treatment, cells were washed twice with PBS and fixed in absolute ice-cold methanol for 20 minutes at –20°C and then rinsed in ice-cold acetone for 20 seconds. Following three washes with PBS, the preparations were incubated with 0.5% NP40 for 20 minutes at room temperature. After fixation, the cells were washed 3 times with 5-minute incubations with PBS and finally blocked with 2%BSA/1% donkey serum in PBS for 1 hour at room temperature. The cells were incubated overnight at 4^0C with primary antibodies. Antibodies used for immunofluorescence staining of the cells in this study include Rad51 (1:1000; Ab-1), RPA34 (1:1000; Ab-1) from Oncogene Research Products; Ab1801 (1:1000; amino terminus-specific p53 from Novocastra); γ-H2AX (1:500; Cat #23646; Upstate Biotechnology); BRCA1 (1:200; RB-020-PO; Neomarkers Technology) and BRCA2 (1:50; PC146; Oncogene Research Productcs, Inc.)

Cultures incubated solely with 3%BSA as a control to account for non-specific secondary antibody binding. Cultures were then washed with 0.5%BSA/ 0.175%Tween20, incubated with diluted fluorophore-conjugated secondary antibody [either donkey-anti-mouse-rhodamine red X (RRX) or donkey-anti-rabbit-fluorescein isothiocyanate (FITC), (Jackson Immunoresearch)] for 45 minutes, and further washed with 0.5%BSA/ 0.175%Tween20. Finally, cultures were counter-stained with 0.1ug/ml diamidinophenyl-indole (DAPI) for 10 minutes, washed with 1x PBS, and mounted in Vectashield media to decrease the rate of photo-bleaching of the fluorophores for subsequent analysis using confocal microscopy.

Confocal microscopy and image analyses

Images were captured using a dual channel Zeiss LSM510 laser scanning confocal microscope equipped with a krypton/argon laser and the corresponding dichromic reflectors (Bio-Rad Laboratories) with a final magnification of 630X, obtained from optical sections of 1.8um thickness, and with a pixel density of 512 X 512 pixels per image. Excitation and absorption settings used to detect the various fluorophores are as follows: RRX (ie. 543nm, LP560nm), FITC (ie. 488nm, BP505-530nm), and

DAPI (ie. 351nm, 385-470nm). Cells were imaged under conditions of equivalent pinhole and black level settings. The gain was adjusted for each image to ensure that the pixel values in each section were not maximal and, therefore, not saturating. Fluorescence signals were amplified and fed into a multiparameter image analysis program. Quantitative data reported are based on at least three replicate experiments in which 25-50 nuclei for each fibroblast strain, dose, and time point were exported and analysed using Adobe Photoshop 5.5 or the Northern Eclipse image analysis program. The images were colored electronically (green for FITC and blue for DAPI labeling). The image were then merged electronically with light blue staining representing the merging of the blue and green labeling, indicating localization of Rad51 in the nucleus. Results reported here are based on visual observation of discrete nuclear foci. The calculated value represents the mean and 95%CIs of at least two independent experiments and 30-50 cells counted per samples. These foci were determined based on their intensities above threshold intensity values of background staining. The data is presented either as the mean total number of foci per nucleus or as a percentage of total nuclei that are foci-positive nuclei (ie. nuclei with greater than 2 foci). The latter definition of IRIF-positive nuclei was chosen on the basis of previous studies for comparative purposes and based on the initial comparison with non-irradiated control cultures that had background punctate stains of less than three foci. Other parameters collected included size and intensity of IRIF and the fluorescent total intensity, FTI, of the IRIF relative to the area of DAPI-staining within the nucleus.

Immunohistochemistry (IHC) of Prostate Xenografts and Primary Human Biopsies

For xenograft studies, 1 x 10^6 PC3 cells were injected i.m. into the gastronemius musle of the hing leg of Balbc/nu mice. The *in vivo* tumor doubling (T_d) time of this xenograft is 4 days (Meng and Bristow, unpublished). Tumors were mock-irradiated or irradiated at a weight of 0.5 gms with 20 Gy using a 250KvP X-ray unit without anaesthesia. For irradiation, the mouse was lightly restrained in a lucite holder box with lead shielding, such that only the tumor-bearing hind leg was within the irradiation volume. Tumors were excised from mock-irradiated and irradiated and placed immediately in formalin for subsequent fixation and immunostaining using primary Rad51 (Ab-1, Oncogene Research Products) and secondary horseradish peroxidase (HRP) antibodies for immunodetection. A similar IHC protocol was used on selected human prostate cancer biopsies taken at the time of prostate cancer diagnosis at the Princess Margaret Hospital. All studies were in ethical compliance with the PMH Animal Care Committee and PMH human Research Ethics Board guidelines.

REFERENCES:

(*1*) Falck J, Petrini JH, Williams BR, Lukas J, Bartek J. The DNA damage-dependent intra-S phase checkpoint is regulated by parallel pathways. Nat Genet 2002;30:290-4.

(*2*) Chang BD, Swift ME, Shen M, Fang J, Broude EV, Roninson IB. Molecular determinants of terminal growth arrest induced in tumor cells by a chemotherapeutic agent. Proc Natl Acad Sci U S A 2002;99:389-94.

(*3*) Roninson IB, Broude EV, Chang BD. If not apoptosis, then what? Treatment-induced senescence and mitotic catastrophe in tumor cells. Drug Resist Updat 2001;4:303-13.

(*4*) Kote-Jarai Z, Eeles RA. BRCA1, BRCA2 and their possible function in DNA damage response. Br J Cancer 1999;81:1099-102.

(*5*) Venkitaraman AR. Functions of BRCA1 and BRCA2 in the biological response to DNA damage. J Cell Sci 2001;114:3591-8.

(*6*) Venkitaraman AR. Cancer susceptibility and the functions of BRCA1 and BRCA2. Cell 2002;108:171-82.

(*7*) Moynahan ME, Pierce AJ, Jasin M. BRCA2 is required for homology-directed repair of chromosomal breaks. Mol Cell 2001;7:263-72.

(*8*) Dasika GK, Lin SC, Zhao S, Sung P, Tomkinson A, Lee EY. DNA damage-induced cell cycle checkpoints and DNA strand break repair in development and tumorigenesis. Oncogene 1999;18:7883-99.

(*9*) van Gent DC, Hoeijmakers JH, Kanaar R. Chromosomal stability and the DNA double-stranded break connection. Nat Rev Genet 2001;2:196-206.

(*10*) Thompson LH, Schild D. Homologous recombinational repair of DNA ensures mammalian chromosome stability. Mutat Res 2001;477:131-53.

(*11*) Verkaik NS, Esveldt-van Lange RE, van Heemst D, Bruggenwirth HT, Hoeijmakers JH, Zdzienicka MZ, et al. Different types of V(D)J recombination and end-joining defects in DNA double-strand break repair mutant mammalian cells. Eur J Immunol 2002;32:701-9.

(*12*) Wang H, Zeng ZC, Bui TA, Sonoda E, Takata M, Takeda S, et al. Efficient rejoining of radiation-induced DNA double-strand breaks in vertebrate cells deficient in genes of the RAD52 epistasis group. Oncogene 2001;20:2212-24.

(*13*) Bishay K, Ory K, Olivier MF, Lebeau J, Levalois C, Chevillard S. DNA damage-related RNA expression to assess individual sensitivity to ionizing radiation. Carcinogenesis 2001;22:1179-83.

(*14*) French CA, Masson JY, Griffin CS, O'Regan P, West SC, Thacker J. Role of mammalian RAD51L2 (RAD51C) in recombination and genetic stability. J Biol Chem 2002;277:19322-30.

(*15*) Masson JY, Tarsounas MC, Stasiak AZ, Stasiak A, Shah R, McIlwraith MJ, et al. Identification and purification of two distinct complexes containing the five RAD51 paralogs. Genes Dev 2001;15:3296-307.

(*16*) Takata M, Sasaki MS, Tachiiri S, Fukushima T, Sonoda E, Schild D, et al. Chromosome instability and defective recombinational repair in knockout mutants of the five Rad51 paralogs. Mol Cell Biol 2001;21:2858-66.

(*17*) Essers J, Houtsmuller AB, van Veelen L, Paulusma C, Nigg AL, Pastink A, et al. Nuclear dynamics of RAD52 group homologous recombination proteins in response to DNA damage. Embo J 2002;21:2030-7.

(*18*) Kraakman-van der Zwet M, Overkamp WJ, van Lange RE, Essers J, van Duijn-Goedhart A, Wiggers I, et al. Brca2 (XRCC11) deficiency results in radioresistant DNA synthesis and a higher frequency of spontaneous deletions. Mol Cell Biol 2002;22:669-79.

(*19*) Lambert S, Lopez BS. Role of RAD51 in sister-chromatid exchanges in mammalian cells. Oncogene 2001;20:6627-31.
(*20*) Lambert S, Lopez BS. Inactivation of the RAD51 recombination pathway stimulates UV-induced mutagenesis in mammalian cells. Oncogene 2002;21:4065-9.
(*21*) Daboussi F, Dumay A, Delacote F, Lopez B. DNA double-strand break repair signalling: The case of RAD51 post-translational regulation. Cell Signal 2002;14:969.
(*22*) Scully R, Puget N, Vlasakova K. DNA polymerase stalling, sister chromatid recombination and the BRCA genes. Oncogene 2000;19:6176-83.
(*23*) Sharan SK, Morimatsu M, Albrecht U, Lim DS, Regel E, Dinh C, et al. Embryonic lethality and radiation hypersensitivity mediated by Rad51 in mice lacking Brca2. Nature 1997;386:804-10.
(*24*) Hajibagheri MA. Visualization of DNA and RNA molecules, and protein-DNA complexes for electron microscopy. Mol Biotechnol 2000;15:167-84.
(*25*) Raderschall E, Golub EI, Haaf T. Nuclear foci of mammalian recombination proteins are located at single-stranded DNA regions formed after DNA damage. Proc Natl Acad Sci U S A 1999;96:1921-6.
(*26*) Bassing CH, Chua KF, Sekiguchi J, Suh H, Whitlow SR, Fleming JC, et al. Increased ionizing radiation sensitivity and genomic instability in the absence of histone H2AX. Proc Natl Acad Sci U S A 2002;99:8173-8.
(*27*) Modesti M, Kanaar R. DNA repair: spot(light)s on chromatin. Curr Biol 2001;11:R229-32.
(*28*) Haaf T, Raderschall E, Reddy G, Ward DC, Radding CM, Golub EI. Sequestration of mammalian Rad51-recombination protein into micronuclei. J Cell Biol 1999;144:11-20.
(*29*) Godthelp BC, Artwert F, Joenje H, Zdzienicka MZ. Impaired DNA damage-induced nuclear Rad51 foci formation uniquely characterizes Fanconi anemia group D1. Oncogene 2002;21:5002-5.
(*30*) Carling T, Imanishi Y, Gaz RD, Arnold A. RAD51 as a candidate parathyroid tumour suppressor gene on chromosome 15q: absence of somatic mutations. Clin Endocrinol (Oxf) 1999;51:403-7.
(*31*) Fan S, Wang JA, Yuan RQ, Ma YX, Meng Q, Erdos MR, et al. BRCA1 as a potential human prostate tumor suppressor: modulation of proliferation, damage responses and expression of cell regulatory proteins. Oncogene 1998;16:3069-82.
(*32*) Hilton JL, Geisler JP, Rathe JA, Hattermann-Zogg MA, DeYoung B, Buller RE. Inactivation of BRCA1 and BRCA2 in ovarian cancer. J Natl Cancer Inst 2002;94:1396-406.
(*33*) Kato M, Yano K, Matsuo F, Saito H, Katagiri T, Kurumizaka H, et al. Identification of Rad51 alteration in patients with bilateral breast cancer. J Hum Genet 2000;45:133-7.
(*34*) Rauh-Adelmann C, Lau KM, Sabeti N, Long JP, Mok SC, Ho SM. Altered expression of BRCA1, BRCA2, and a newly identified BRCA2 exon 12 deletion variant in malignant human ovarian, prostate, and breast cancer cell lines. Mol Carcinog 2000;28:236-46.
(*35*) Rosen EM, Fan S, Goldberg ID. BRCA1 and prostate cancer. Cancer Invest 2001;19:396-412.
(*36*) Yuan R, Fan S, Wang JA, Meng Q, Ma Y, Schreiber D, et al. Coordinate alterations in the expression of BRCA1, BRCA2, p300, and Rad51 in response to genotoxic and other stresses in human prostate cancer cells. Prostate 1999;40:37-49.
(*37*) Bhattacharyya A, Ear US, Koller BH, Weichselbaum RR, Bishop DK. The breast cancer susceptibility gene BRCA1 is required for subnuclear assembly of Rad51 and survival following treatment with the DNA cross-linking agent cisplatin. J Biol Chem 2000;275:23899-903.
(*38*) Chen J, Silver DP, Walpita D, Cantor SB, Gazdar AF, Tomlinson G, et al. Stable interaction between the products of the BRCA1 and BRCA2 tumor suppressor genes in mitotic and meiotic cells. Mol Cell 1998;2:317-28.

(*39*) Chen JJ, Silver D, Cantor S, Livingston DM, Scully R. BRCA1, BRCA2, and Rad51 operate in a common DNA damage response pathway. Cancer Res 1999;59:1752s-6s.

(*40*) Yang H, Jeffrey PD, Miller J, Kinnucan E, Sun Y, Thoma NH, et al. BRCA2 function in DNA binding and recombination from a BRCA2-DSS1-ssDNA structure. Science 2002;297:1837-48.

(*41*) Chen CF, Chen PL, Zhong Q, Sharp ZD, Lee WH. Expression of BRC repeats in breast cancer cells disrupts the BRCA2-Rad51 complex and leads to radiation hypersensitivity and loss of G(2)/M checkpoint control. J Biol Chem 1999;274:32931-5.

(*42*) Chen PL, Chen CF, Chen Y, Xiao J, Sharp ZD, Lee WH. The BRC repeats in BRCA2 are critical for RAD51 binding and resistance to methyl methanesulfonate treatment. Proc Natl Acad Sci U S A 1998;95:5287-92.

(*43*) Liu Y, West SC. Distinct functions of BRCA1 and BRCA2 in double-strand break repair. Breast Cancer Res 2002;4:9-13.

(*44*) Sarkisian CJ, Master SR, Huber LJ, Ha SI, Chodosh LA. Analysis of murine Brca2 reveals conservation of protein-protein interactions but differences in nuclear localization signals. J Biol Chem 2001;276:37640-8.

(*45*) Xia F, Taghian DG, DeFrank JS, Zeng ZC, Willers H, Iliakis G, et al. Deficiency of human BRCA2 leads to impaired homologous recombination but maintains normal nonhomologous end joining. Proc Natl Acad Sci U S A 2001;98:8644-9.

(*46*) Chen G, Yuan SS, Liu W, Xu Y, Trujillo K, Song B, et al. Radiation-induced assembly of Rad51 and Rad52 recombination complex requires ATM and c-Abl. J Biol Chem 1999;274:12748-52.

(*47*) Chodosh LA. Expression of BRCA1 and BRCA2 in normal and neoplastic cells. J Mammary Gland Biol Neoplasia 1998;3:389-402.

(*48*) Davies AA, Masson JY, McIlwraith MJ, Stasiak AZ, Stasiak A, Venkitaraman AR, et al. Role of BRCA2 in control of the RAD51 recombination and DNA repair protein. Mol Cell 2001;7:273-82.

(*49*) Marmorstein LY, Ouchi T, Aaronson SA. The BRCA2 gene product functionally interacts with p53 and RAD51. Proc Natl Acad Sci U S A 1998;95:13869-74.

(*50*) Saintigny Y, Dumay A, Lambert S, Lopez BS. A novel role for the Bcl-2 protein family: specific suppression of the RAD51 recombination pathway. Embo J 2001;20:2596-607.

(*51*) Saintigny Y, Lopez BS. Homologous recombination induced by replication inhibition, is stimulated by expression of mutant p53. Oncogene 2002;21:488-92.

(*52*) Stewart G, Elledge SJ. The two faces of BRCA2, a FANCtastic discovery. Mol Cell 2002;10:2-4.

(*53*) Maacke H, Jost K, Opitz S, Miska S, Yuan Y, Hasselbach L, et al. DNA repair and recombination factor Rad51 is over-expressed in human pancreatic adenocarcinoma. Oncogene 2000;19:2791-5.

(*54*) Raderschall E, Stout K, Freier S, Suckow V, Schweiger S, Haaf T. Elevated levels of Rad51 recombination protein in tumor cells. Cancer Res 2002;62:219-25.

(*55*) Yanagisawa T, Urade M, Yamamoto Y, Furuyama J. Increased expression of human DNA repair genes, XRCC1, XRCC3 and RAD51, in radioresistant human KB carcinoma cell line N10. Oral Oncol 1998;34:524-8.

(*56*) Bosken CH, Wei Q, Amos CI, Spitz MR. An analysis of DNA repair as a determinant of survival in patients with non-small-cell lung cancer. J Natl Cancer Inst 2002;94:1091-9.

(*57*) Slupianek A, Schmutte C, Tombline G, Nieborowska-Skorska M, Hoser G, Nowicki MO, et al. BCR/ABL regulates mammalian RecA homologs, resulting in drug resistance. Mol Cell 2001;8:795-806.

(*58*) Wang ZM, Chen ZP, Xu ZY, Christodoulopoulos G, Bello V, Mohr G, et al. In vitro evidence for homologous recombinational repair in resistance to melphalan. J Natl Cancer Inst 2001;93:1473-8.

(*59*) Vispe S, Cazaux C, Lesca C, Defais M. Overexpression of Rad51 protein stimulates homologous recombination and increases resistance of mammalian cells to ionizing radiation. Nucleic Acids Res 1998;26:2859-64.

(*60*) Kim PM, Allen C, Wagener BM, Shen Z, Nickoloff JA. Overexpression of human RAD51 and RAD52 reduces double-strand break-induced homologous recombination in mammalian cells. Nucleic Acids Res 2001;29:4352-60.

(*61*) Larminat F, Germanier M, Papouli E, Defais M. Deficiency in BRCA2 leads to increase in non-conservative homologous recombination. Oncogene 2002;21:5188-92.

(*62*) Yanez RJ, Porter AC. Differential effects of Rad52p overexpression on gene targeting and extrachromosomal homologous recombination in a human cell line. Nucleic Acids Res 2002;30:740-8.

(*63*) Carlomagno F, Burnet NG, Turesson I, Nyman J, Peacock JH, Dunning AM, et al. Comparison of DNA repair protein expression and activities between human fibroblast cell lines with different radiosensitivities. Int J Cancer 2000;85:845-9.

(*64*) Spain BH, Larson CJ, Shihabuddin LS, Gage FH, Verma IM. Truncated BRCA2 is cytoplasmic: implications for cancer-linked mutations. Proc Natl Acad Sci U S A 1999;96:13920-5.

(*65*) Yuan SS, Lee SY, Chen G, Song M, Tomlinson GE, Lee EY. BRCA2 is required for ionizing radiation-induced assembly of Rad51 complex in vivo. Cancer Res 1999;59:3547-51.

(*66*) Choudhary SK, Li R. BRCA1 modulates ionizing radiation-induced nuclear focus formation by the replication protein A p34 subunit. J Cell Biochem 2002;84:666-74.

(*67*) Kitao H, Yuan ZM. Regulation of ionizing radiation-induced Rad52 nuclear foci formation by c-Abl-mediated phosphorylation. J Biol Chem 2002;11:11.

(*68*) De Potter CR, Coene ED, Schelfhout VR. Localization of BRCA1 protein at the cellular level. J Mammary Gland Biol Neoplasia 1998;3:423-9.

(*69*) Gonzalez R, Silva JM, Dominguez G, Garcia JM, Martinez G, Vargas J, et al. Detection of loss of heterozygosity at RAD51, RAD52, RAD54 and BRCA1 and BRCA2 loci in breast cancer: pathological correlations. Br J Cancer 1999;81:503-9.

(*70*) Shen CY, Yu JC, Lo YL, Kuo CH, Yue CT, Jou YS, et al. Genome-wide search for loss of heterozygosity using laser capture microdissected tissue of breast carcinoma: an implication for mutator phenotype and breast cancer pathogenesis. Cancer Res 2000;60:3884-92.

(*71*) Collis SJ, Tighe A, Scott SD, Roberts SA, Hendry JH, Margison GP. Ribozyme minigene-mediated RAD51 down-regulation increases radiosensitivity of human prostate cancer cells. Nucleic Acids Res 2001;29:1534-8.

(*72*) Taki T, Ohnishi T, Yamamoto A, Hiraga S, Arita N, Izumoto S, et al. Antisense inhibition of the RAD51 enhances radiosensitivity. Biochem Biophys Res Commun 1996;223:434-8.

(*73*) Bristow RG, Hu Q, Jang A, Chung S, Peacock J, Benchimol S, et al. Radioresistant MTp53-expressing rat embryo cell transformants exhibit increased DNA-dsb rejoining during exposure to ionizing radiation. Oncogene 1998;16:1789-802.

FIGURE LEGENDS:

Figure 1.
(a) Sample RNAase protection assay of ATM/p53-related stress response pathways. ^{32}P labeled multi-riboprobes were hybridized to the total mRNA derived from mock-irradiated and irradiated (10Gy-4hrs) asynchronously growing cells. Single-strand specific nucleases are added to digest any unhybridized probe and sample RNA. The probe-protected RNA species are separated via electrophoresis and quantified by relative densitometry as detailed in the Methods. Specific multiprobes used in this analysis are indicated in the far left margin of the blot aside the corresponding gene band of interest. Lane assignments of mRNA probed from non-irradiated (odd lane numbers) and irradiated (even lane numbers) are as follows: lanes 1 and 2: LNCaP; lanes 3 and 4: PC3; lanes 5 and 6: DU145; lanes 7 and 8: PREC; lanes 9 and 10: PRSC; lane 11, Hela cell positive control; lane 12, yeast negative control and lane 13, RNA probes. GAPDH was a housekeeping gene that served as internal control for densitometric quantitation of results. Note IR-induced $p21^{WAF}$ signal in WT-p53 expressing PrSC, PrEC and LNcaP cell lines consistent with previous data from our lab supporting an intact IR-induced G1 checkpoint in these cells.
(b) Quantitation of ATM/p53-dependent stress response gene expression based on RPA analyses in normal and malignant prostate cells: upper figure shows basal (ie non-irradiated) levels of mRNA expression and lower panel shows expression of same genes at 4 hours following 10 Gy Significantly increased expression was observed for the p21WAF gene in WTp53-expressing cells (PrSC, PrEC, LNCaP) which was time- and dose-dependent (data not shown). The bax, bcl-2 and gadd45 gene expression in these cell lines was also significantly increased post-IR ($p<0.05$). For all RPA analyses, shown are the mean gene expression +/- 1 S.E.; based on 2-3 independent experiments.

Figure 2:
Quantitation of NHEJ pathway-related, gene expression based on RPA analyses in normal and malignant prostate cells: upper figure shows basal (ie non-irradiated) levels of mRNA expression and lower panel shows expression of same genes at 4 hours following 10 Gy. Ku70 and Ku80 genes are overexpressed in all cells in comparison to other NHEJ genes. There was little evidence of IR-induction for any NHEJ gene. Both RPA and Western blot data (see insert) confirms increased mRNA and protein expression of Ku70 by ~2-3 fold in the malignant cells when compared to normal cells, in both basal and post-irradiation plots. Ku70 protein expression was not further increased with radiation (Western blot data for 10Gy-4hrs; data not shown).

Figure 3:
(a) HR pathway-related gene expression based on RPA analyses in normal and malignant prostate cells: upper figure shows basal (ie non-irradiated) levels of mRNA expression and lower panel shows expression of same genes at 4 hours following 10 Gy. IR-induction was observed for the Rad51, Rad54, Rad52 and XRCC3 genes in the PrSC stromal cell line ($P<0.05$), but no statistically significant IR-induced gene expression was observed for the epithelial cell lines. Note statistically increased expression of Rad51, Rad54, Rad52 and XRCC3 in malignant cell lines in comparison to normal cell cultures based on both basal and post-irradiation data ($P<0.05$).
(b) Confirmation of increased basal Rad51, Rad54 and XRCC3 protein expression in malignant prostate cells using Western blots analysis. Quantitative densitometry was based Western blots similar to the one shown in upper panel to derive the values of protein expression quantitated in the lower panel. HR-related protein expression was not further induced at 4 hours following a dose 10Gy (data not shown).

Figure 4.
(a) Imunofluorescent confocal micrographs of normal and malignant prostate cells showing induction of punctuate, intranuclear foci (ie IRIF) of DNA-break sensor, γH2AX protein, at 4 hours following a dose of 10 Gy. The cells were fixed and immunostained with a primary γ–H2AX antibody and a fluorescein isothicyanate (FITC-green)-conjugated, secondary antibody. The cells were counterstained with the nuclear dye, DAPI (blue). Representative confocal fluorescent images were collected and analyzed with the use of the northern Eclipse image analysis system. Note increased IRIF formation post-irradiation in all cell lines including Capan-1 pancreatic cell line which expresses a BRCA2 truncated protein (ie BRCA2-defective) and can not form Rad51 nor BRCA2 IRIF. Increased baseline γH2AX IRIF (ie pre-irradiation) has been reported previously and was elevated in malignant cell lines(*27*).
(b) Quantification of the number of γH2AX IRIF per cell nucleus in cell panel based on counting 25-50 cells per experiment showing similar γH2AX IRIF responses within all 5 cell lines.
(c) Quantification of the number of cells positive for 3 or more γH2AX IRIF within the cell panel showing similar percentages of cells have an intact γH2AX IRIF response

Figure 5.
(a) Control immunofluorescent confocal micrographs of irradiated (10Gy-24hrs) and non-irradiated GM05757 human fibroblasts showing increased γH2AX(green-FITC) & Mre11(red-Rhodamine) IRIF (upper panel) and Rad51(Green-FITC) & RPA(Red-Rhodamine) IRIF (lower panel) following 10Gy. DAPI staining is shown to outline cell nucleus. Following superimposition of images for a given cell nucleus, both Mre11 and γH2AX IRIF and Rad51 and RPA IRIF, co-localize (yellow fluorescence) at sites of DNA damage supporting the use of the Oncogene Ab-1 Rad51 antibodies in IRIF experiments.
(b) Imunofluorescent confocal micrographs of GM05757 fibroblasts (control) and PrSC and PrEC prostate cells showing induction of punctuate, intranuclear Rad51 foci (ie IRIF) at 4 hours following a dose of 10 Gy. Note increased number and size of IRIF in all 3 cell lines post-irradiation. PrEC cells consistently had high levels of cytoplasmic Rad51 staining when compared to GM05757 and PrSC stromal cells. Following irradiation, peri-nuclear clearing of Rad51 staining appeared in PrEC cells.
(c) Imunofluorescent confocal micrographs of malignant prostate cells and Capan-1cells (ie. BRCA2- and Rad51-IRIF negative control) showing minimal induction of Rad51 IRIF in Capan-1, LNCaP and PC3 cells, when compared to DU-145 cells. Note increased peri-nuclear nuclear punctuate staining of Rad51 in the three malignant prostate cell lines following irradiation, suggesting a defect in cytoplasmic to nuclear translocation for Rad51 in PC3 and LNCaP cells.
(d) Quantitation of relative Rad51 IRIF formation over time (upper panel; 4-24 hrs following 10 Gy) and dose (lower panel: 2-10Gy at 4 hrs) between normal (PrEC) and malignant (LNCaP) epithelial prostate cells. The Rad51-IRIF defect in LNCaP cells is independent of dose or time of irradiation.

Figure 6.
(a) Summary quantification of the number of Rad51 IRIF per cell nucleus in cell panel based on counting 25-50 cells per experimental timepoint for malignant and normal cells in panel. Note significant defects ($p<0.05$) in the induction of Rad51 IRIF in LNCaP and PC-3 cells, and minimal IR-induction of Rad51 IRIF beyond baseline in all 3 malignant cell lines, even though all 3 cell lines express ~4-5 fold greater total cellular protein than normal cells. Shown are mean values +/- 1 S.E. for 2-3 independent experiments.
(b) Quantification of the number of cells positive for 3 or more Rad51-IRIF within the cell panel showing significantly ($P<0.05$) decreased percentages of cells that are Rad51 IRIF positive in LNCaP and PC3 cells.

Figure 7.
(a)Imunofluorescent confocal micrographs of normal and malignant prostate cells and Capan-1 control cells showing minimal induction of BRCA2 IRIF in Capan-1, LNCaP and PC3 cells in comparison to DU-145 and normal prostate cells. Similar to Rad51, BRCA2 is cytoplasmic in PC3, LNCaP and Capan-1 cells.
(b) Imunofluorescent confocal micrographs of normal and malignant prostate cells and Capan-1 control cells (ie BRCA2- and Rad51-defective, but not BRCA1-IRIF defective) showing minimal induction of BRCA1 IRIF in LNCaP and PC3 cells, in comparison to Capan-1, DU-145 and normal prostate cells.

Figure 8.
(a) Immunohistochemistry for Rad51 protein within human PC3 cells grown as a solid tumor xenograft in the hind leg of a Balbc/nu mouse following an initial intramuscular injection of 1 x 10^6 cells. Note heterogeneity of cytoplasmic and nuclear staining within tumor prior to irradiation. Following X-irradiation with dose of 20Gy *in vivo*, intratumoural heterogeneity of Rad51 staining is maintained, yet the number and intensity of nuclear staining increases.
(b) Immunohistochemistry for Rad51 protein within a primary human prostate cancer core biopsy consistent with intratumoural heterogeneity and increased nuclear to cytoplasmic Rad51 staining within prostate glands containing malignant cells.

ACKOWLEDGEMENTS:

These studies were supported by the US Army DOD Prostate Cancer Research Program (Grant number DAMD 17-01-1-0110(A-10308)) and the Princess Margaret Hospital Foundation (Prostate Clinical Research Program). We thank S. Al Rashid, A. Meng and F. Jalali for helpful discussions and technical assistance.

Fig. 1a

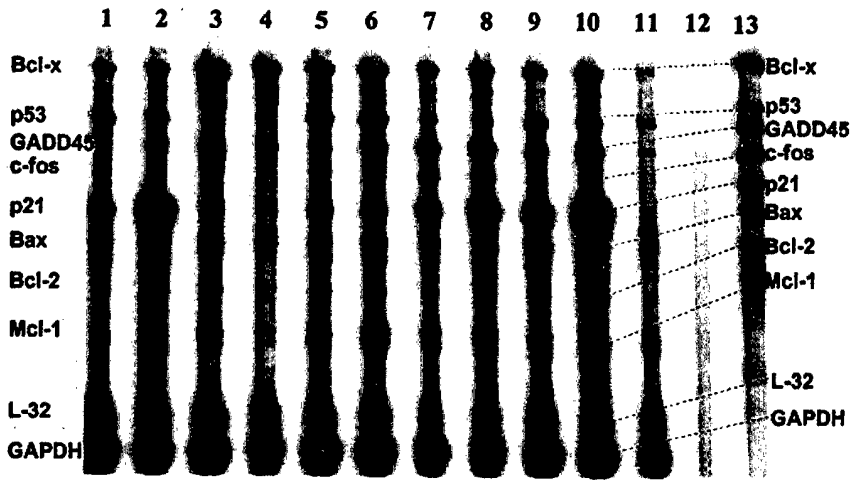
1 2 3 4 5 6 7 8 9 10 11 12 13
Bcl-x
p53
GADD45
c-fos
p21
Bax
Bcl-2
Mcl-1
L-32
GAPDH
Bcl-x
p53
GADD45
c-fos
p21
Bax
Bcl-2
Mcl-1
L-32
GAPDH

Fig 1b

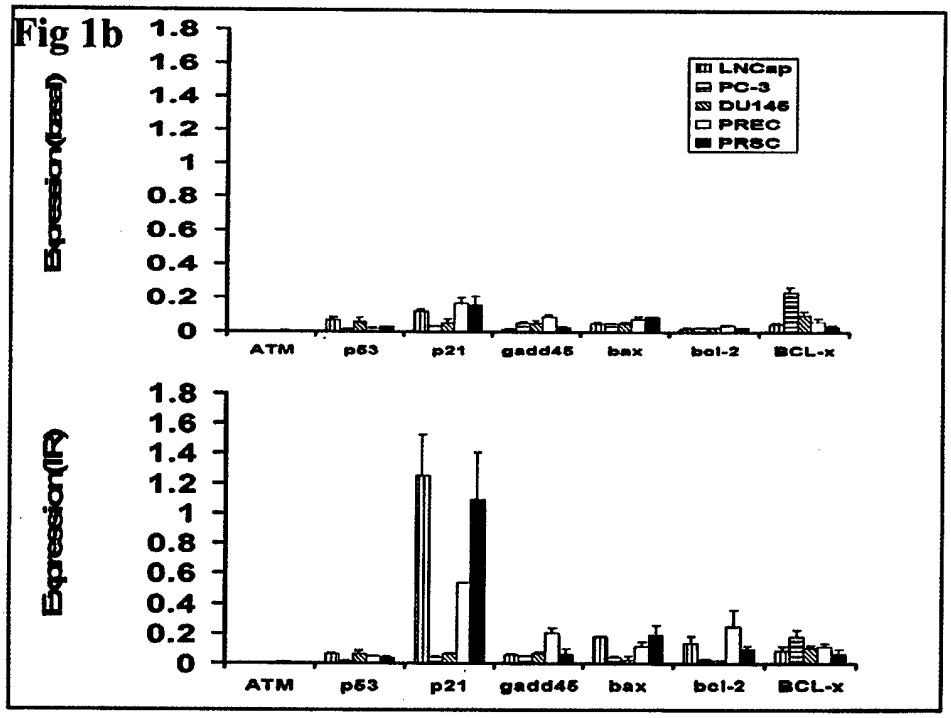
Expression(fold)
1.8
1.6
1.4
1.2
1
0.8
0.6
0.4
0.2
0
LNCap
PC-3
DU145
PREC
PRSC
ATM
p53
p21
gadd45
bax
bcl-2
BCL-x
Expression(IR)
1.8
1.6
1.4
1.2
1
0.8
0.6
0.4
0.2
0
ATM
p53
p21
gadd45
bax
bcl-2
BCL-x

Fig 2

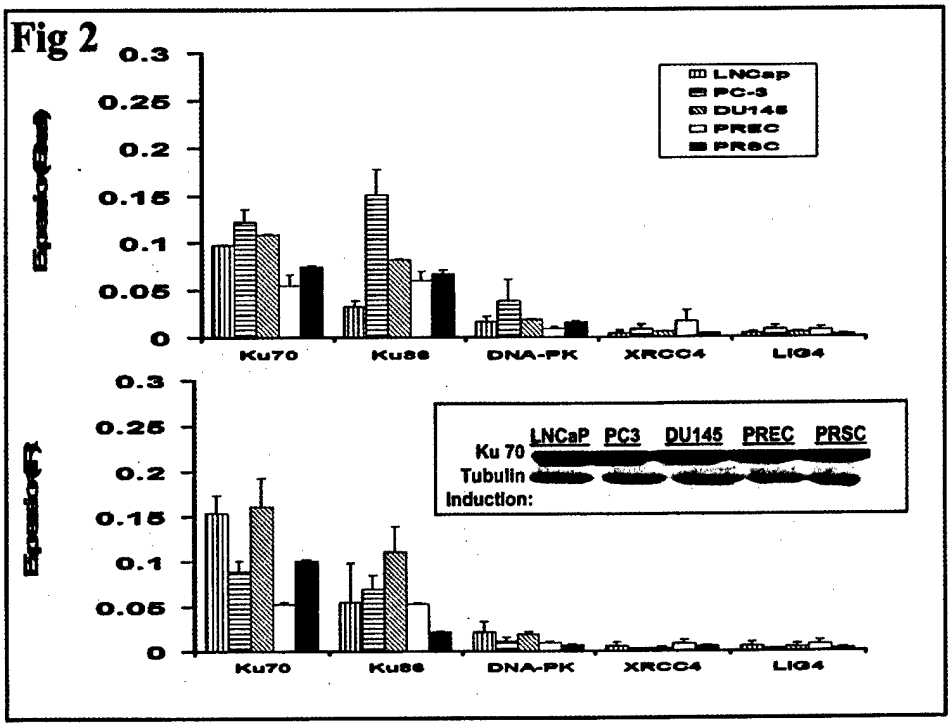
LNCaP
PC-3
DU145
PREC
PRSC
0.3
0.25
0.2
0.15
0.1
0.05
0
Ku70
Ku86
DNA-PK
XRCC4
LIG4
LNCaP PC3 DU145 PREC PRSC
Ku 70
Tubulin
Induction:

Fig.3a

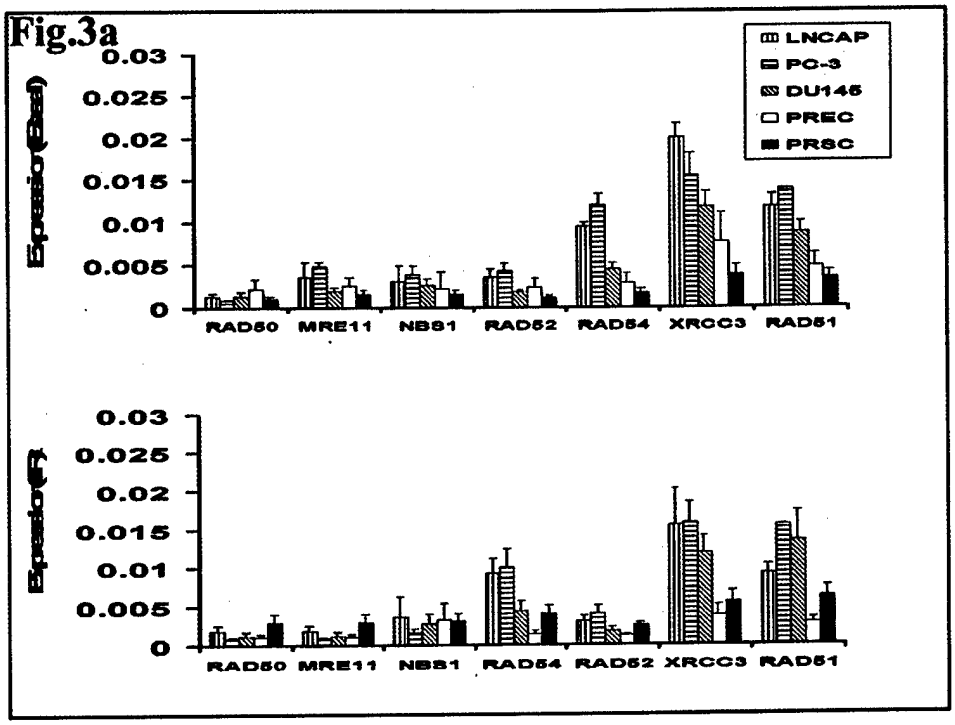
LNCAP
PC-3
DU145
PREC
PRSC
0.03
0.025
0.02
0.015
0.01
0.005
0
RAD50
MRE11
NBS1
RAD52
RAD54
XRCC3
RAD51

Fig.3b

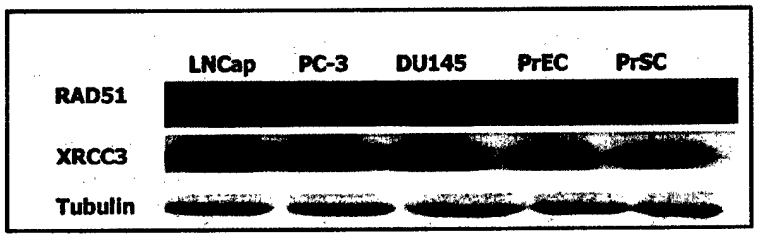
LNCap
PC-3
DU145
PrEC
PrSC
RAD51
XRCC3
Tubulin

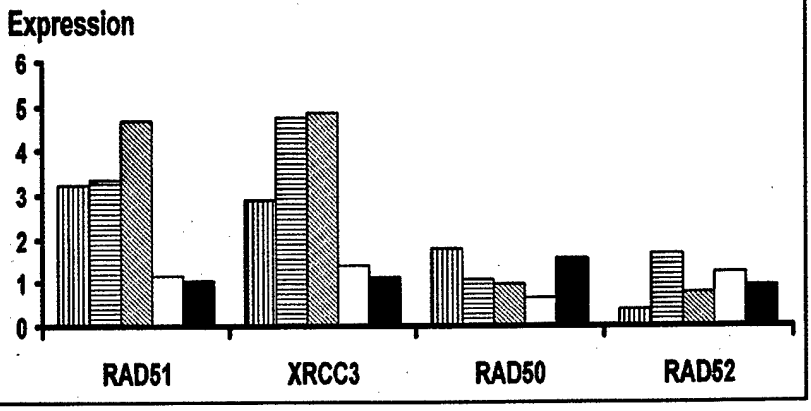
Expression
6
5
4
3
2
1
0
RAD51
XRCC3
RAD50
RAD52

Fig. 4a

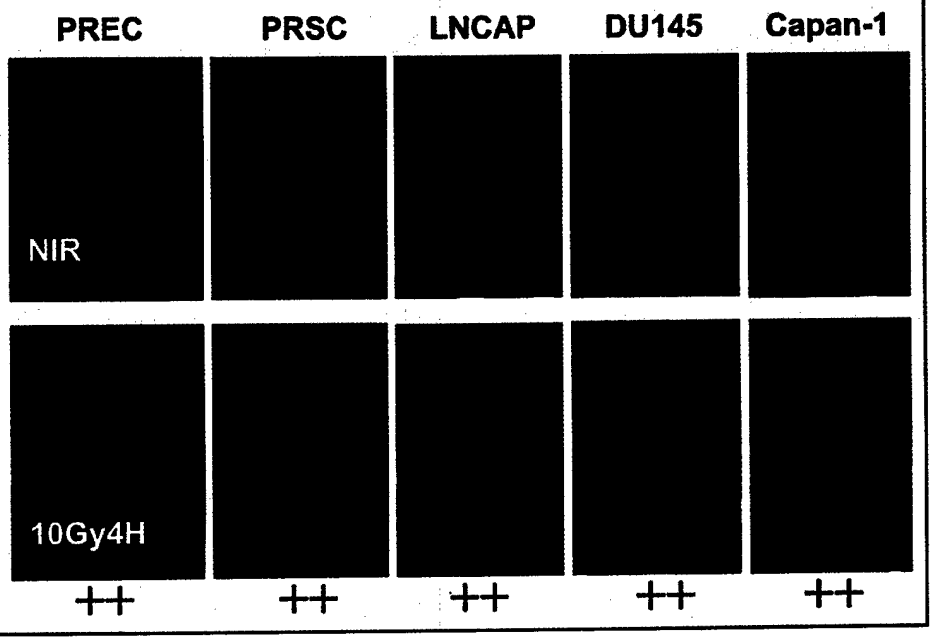
PREC
PRSC
LNCAP
DU145
Capan-1
NIR
10Gy4H
++
++
++
++
++

Fig. 4b

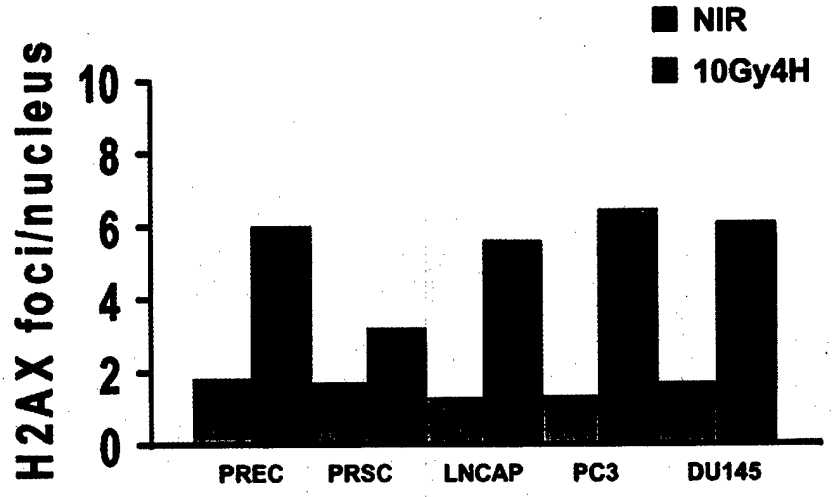
NIR
10Gy4H
H2AX foci/nucleus
10
8
6
4
2
0
PREC
PRSC
LNCAP
PC3
DU145

Fig. 4c

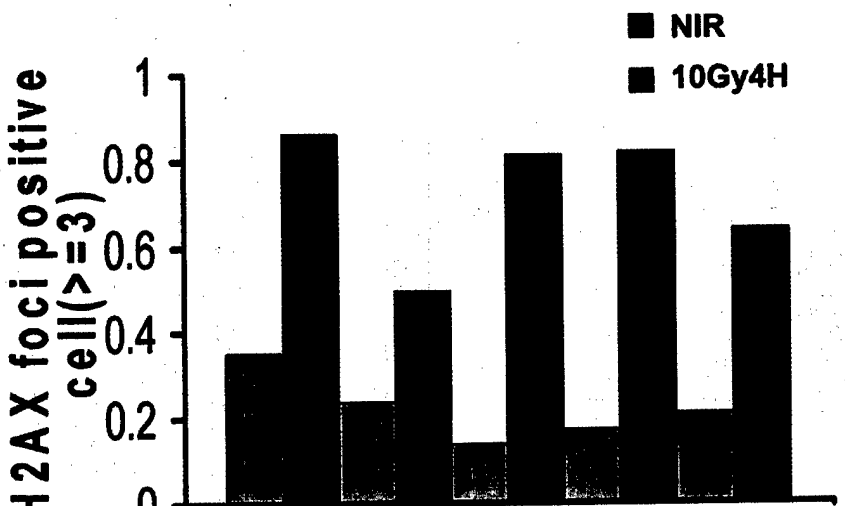
NIR
10Gy4H
H2AX foci positive cell(>=3)
1
0.8
0.6
0.4
0.2
0
PREC
PRSC
LNCAP
PC3
DU145

Fig. 5a

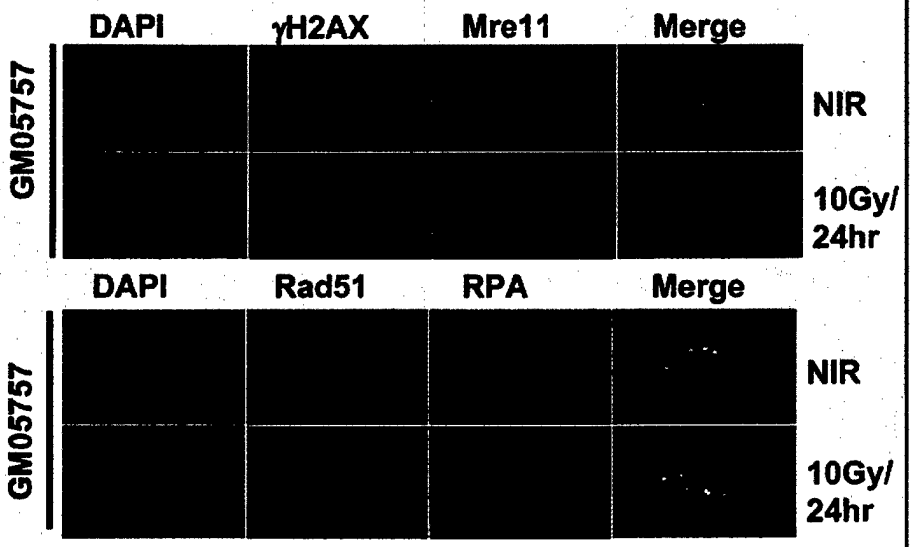
DAPI
γH2AX
Mre11
Merge
GM05757
NIR
10Gy/
24hr
DAPI
Rad51
RPA
Merge
GM05757
NIR
10Gy/
24hr

Fig. 5b

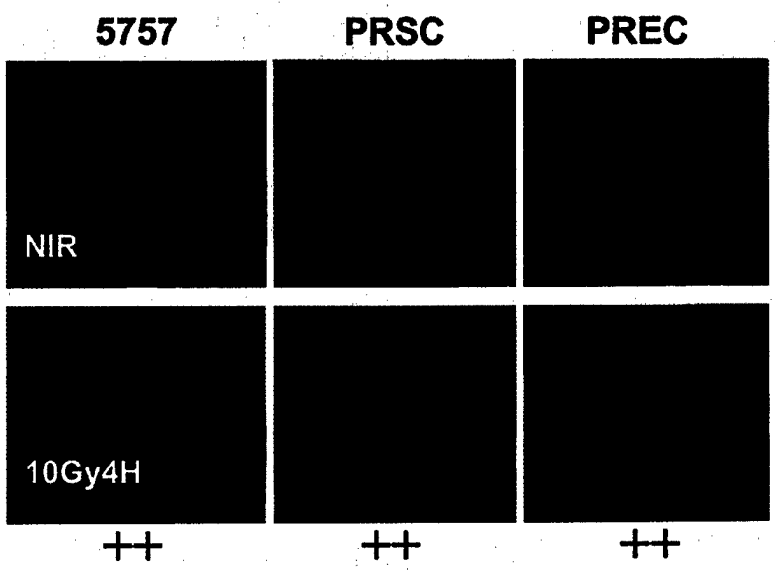
5757
PRSC
PREC
NIR
10Gy4H
++
++
++

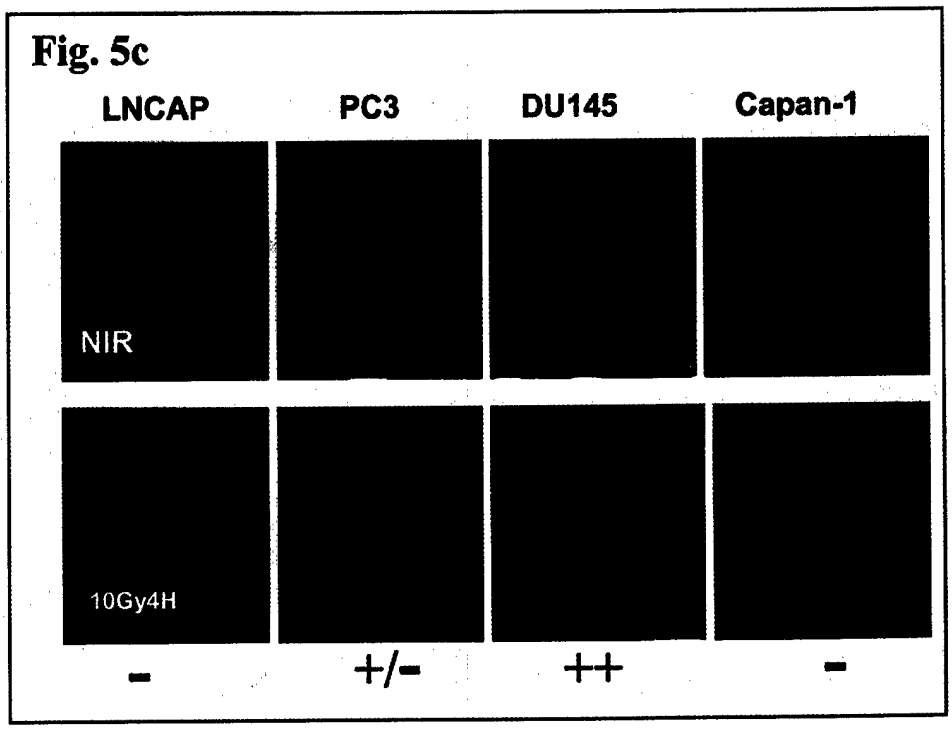
Fig. 5c
LNCAP
PC3
DU145
Capan-1
NIR
10Gy4H
-
+/-
++
-

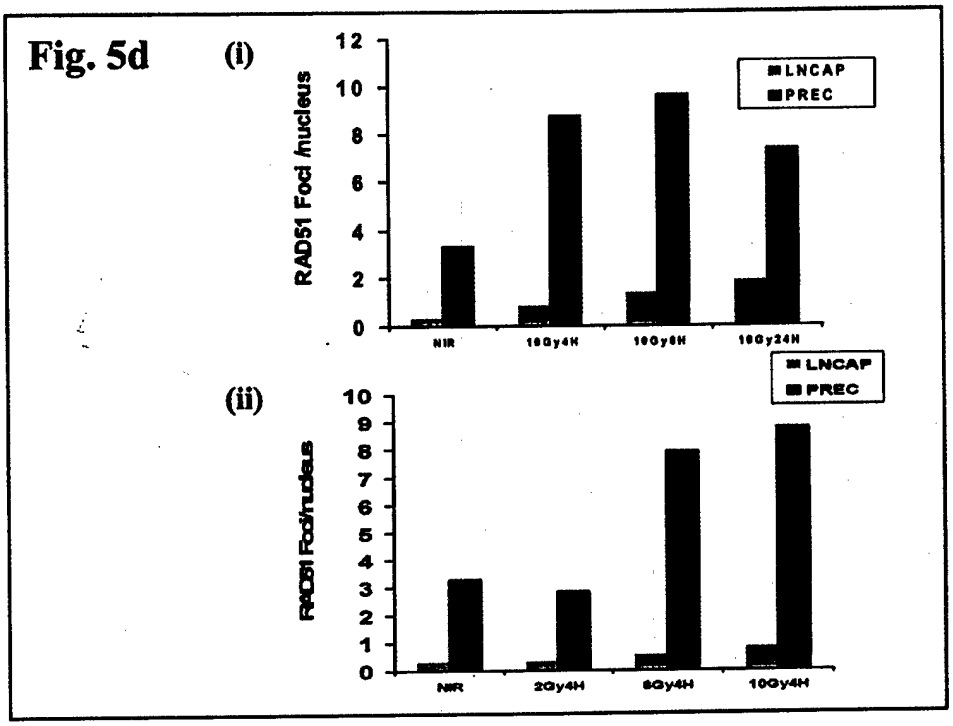
Fig. 5d
(i)
RAD51 Foci /nucleus
12
10
8
6
4
2
0
LNCAP
PREC
NIR
10Gy4H
10Gy8H
10Gy24H
(ii)
RAD51 Foci/nucleus
10
9
8
7
6
5
4
3
2
1
0
LNCAP
PREC
NIR
2Gy4H
6Gy4H
10Gy4H

Fig. 6a

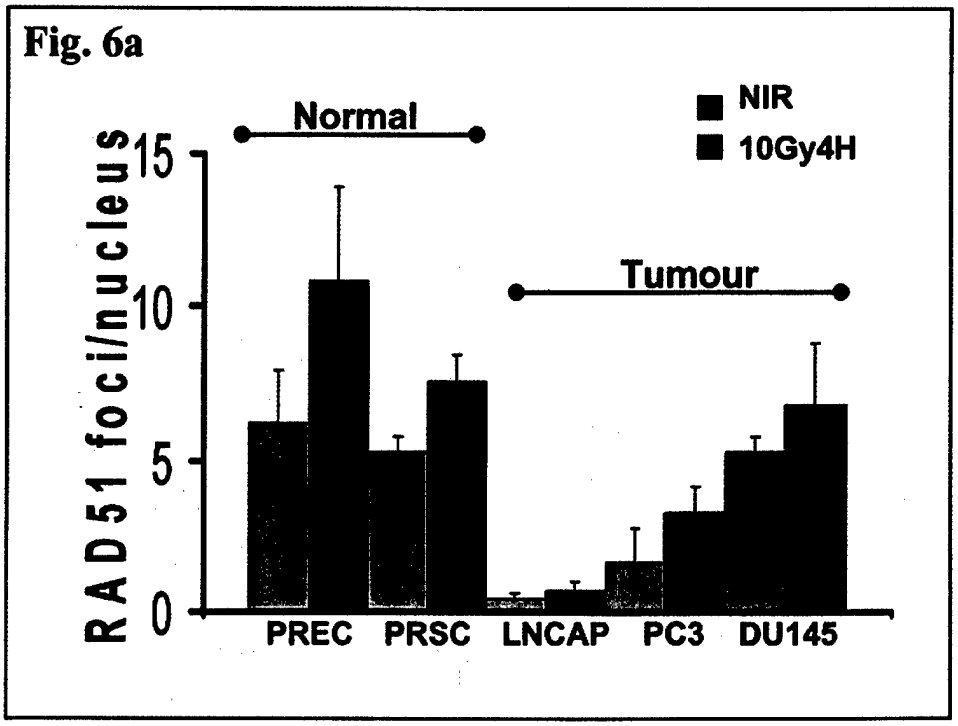
Normal
Tumour
NIR
10Gy4H
RAD51 foci/nucleus
15
10
5
0
PREC
PRSC
LNCAP
PC3
DU145

Fig. 6b

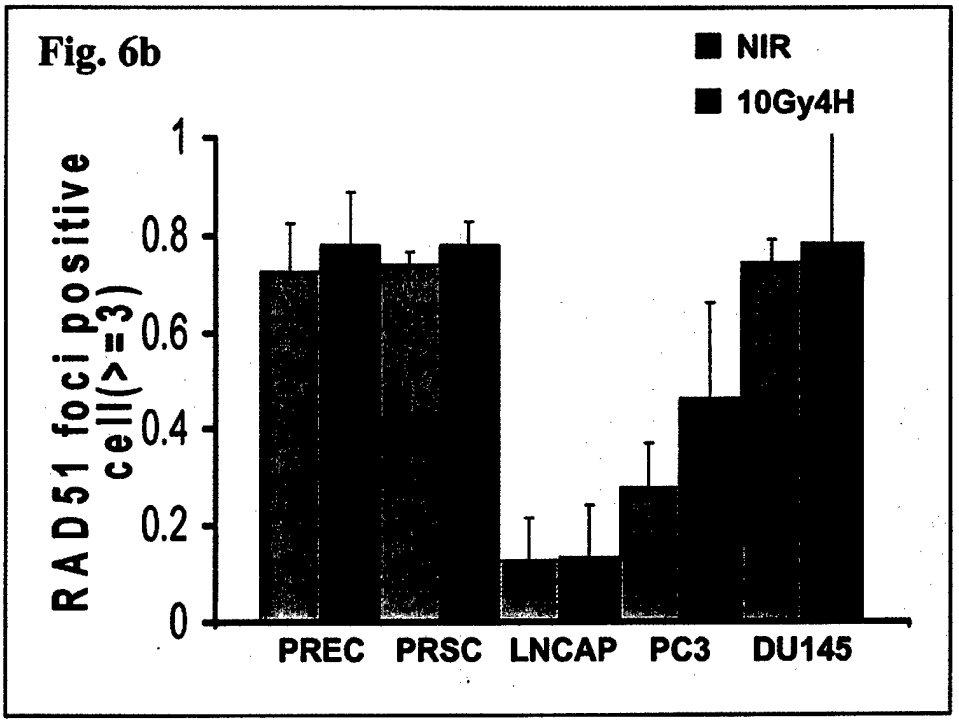
NIR
10Gy4H
RAD51 foci positive cell(>=3)
1
0.8
0.6
0.4
0.2
0
PREC
PRSC
LNCAP
PC3
DU145

Fig. 7a

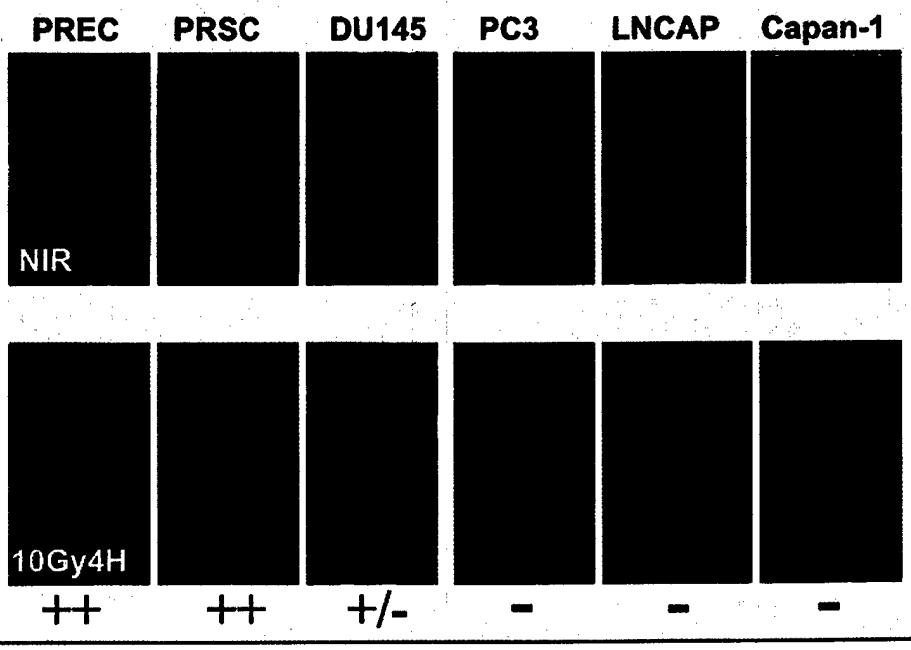
PREC
PRSC
DU145
PC3
LNCAP
Capan-1
NIR
10Gy4H
++
++
+/-
-
-
-

Fig. 7b

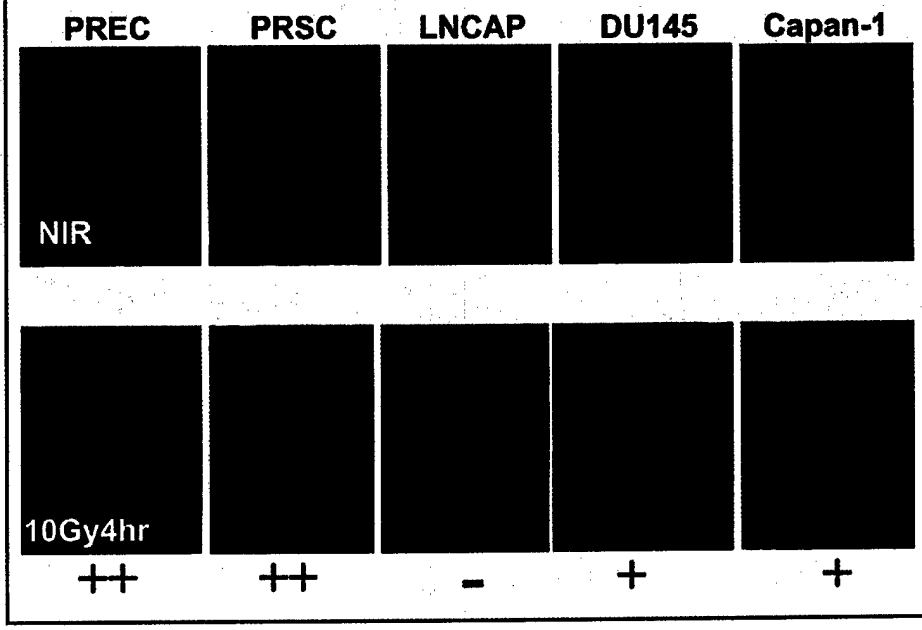
PREC
PRSC
LNCAP
DU145
Capan-1
NIR
10Gy4hr
++
++
-
+
+

Fig. 8

(a)

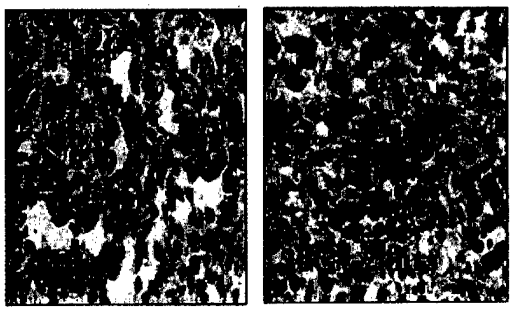

(b)